NASA Technical Memorandum 83196

NASA-TM-83196 19820006677

SPECTRAL ATMOSPHERIC OBSERVATIONS AT NANTUCKET ISLAND, MAY 7-14, 1981

T. A. Talay and L. R. Poole

NOVEMBER 1981

NASA
National Aeronautics and
Space Administration

Langley Research Center
Hampton, Virginia 23665

SUMMARY

During the period May 7-14, 1981, an experiment was conducted by the National Aeronautics and Space Administration, Langley Research Center, on Nantucket Island, Massachusetts, to measure atmospheric optical conditions using a 10-channel solar spectral photometer system. This experiment was part of a larger series of multidisciplinary experiments performed in the area of Nantucket Shoals aimed at studying the dynamics of phytoplankton production processes. Analysis of the collected atmospheric data yielded total and aerosol optical depths, transmittances, normalized sky radiance distributions, and total and sky irradiances. Results of this analysis may aid in atmospheric corrections of remote-sensor data obtained by several sensors overflying the Nantucket Shoals area. Recommendations are presented concerning future experiments using the described solar photometer system and calibration and operational deficiencies uncovered during the experiment.

INTRODUCTION

In remote sensing of the marine environment using multispectral sensors aboard aircraft or spacecraft, the Earth's atmosphere may seriously affect classification or quantification of specific marine features. One can attempt to remove these atmospheric effects through radiative transfer modeling, statistical techniques, or direct atmospheric measurements. Optical properties of the atmosphere which are essential to many atmospheric correction techniques may presently be determined only by accurate atmospheric measurements obtained concurrently during remote-sensing experiments.

During May 1981, a series of aircraft remote-sensing and shipboard in situ experiments were performed in the area of Nantucket Shoals near Nantucket Island, Massachusetts, to study the dynamics of phytoplankton production processes. One experiment objective was to demonstrate the feasibility of using low altitude passive and active remote-sensing techniques to verify, calibrate, and augment Coastal Zone Color Scanner (CZCS) satellite imagery of temperature, chlorophyll, suspended solids, and light attenuation.

To supplement these Nantucket Shoals aircraft remote sensor and shipboard in situ studies, an experiment was conducted by personnel of the NASA Langley Research Center on Nantucket Island to measure atmospheric optical conditions using a 10-channel solar spectral photometer. The purpose of this report is to summarize atmospheric optical depth, radiance, and irradiance measurements made during the period May 7-14, 1981.

TEST SITE

The aircraft remote-sensing and shipboard in situ experiments were conducted in the region of Nantucket Shoals, a topographic high extending some 120 km southwest of the island of Nantucket, Massachusetts, as shown in figure 1. Flight patterns for remote sensor aircraft and cruise tracks for the experiment ships crisscrossed this general area in patterns which were determined by the goals of particular experiments. For measurements of the atmosphere, as described in this report, instruments and associated support equipment were placed at Nantucket Island airport. This land-based placement was as close as practical to the experiment area and allowed stable directional atmospheric measurements which could not be guaranteed aboard moving platforms such as aircraft or ships. The instrument site was on the south side of the island approximately 1.5 km from the shoreline. The instrument view of the sky hemisphere was generally unobstructed except in a northwesterly direction where a low tree line and the experiment support truck obscured a small portion of the sky dome. Compared to the entire sky dome, this interference was considered negligible.

INSTRUMENT DESCRIPTION

Solar and atmospheric radiance and irradiance were measured with a Research Support Instruments (RSI) 10-channel Solar Spectral Photometer. The basic photometer unit and support equipment are shown in figure 2. The photometer is powered by a high voltage source (photometer control unit) and mounted in a two-axis solar tracking table (solar tracker unit) which itself is separately controlled by a solar tracker controller. Data are recorded in digital form (data recorder). The shipping cases shown provide for safe transport only and are not used as a platform for the instrumentation.

Solar Photometer

The Research Support Instruments Solar Spectral Photometer (Model 30-194) is basically a copy of the Scripps Institution of Oceanography's Hand-Held Contrast Reduction Meter (HHCRM) and utilizes a fan-cooled Hamamatsu R928 photomultiplier tube (PMT). The instrument field-of-view for the Nantucket Shoals experiment was 10° total angle. The effects of this angle on the data are described in a later section. Ten 1.27-cm (0.5-in.) diameter interference filters are mounted in a manually rotated filter wheel assembly. The filters were in a wavelength range from 400 to 750 nanometers (nm). Particular characteristics of these filters are presented in table 1. For comparison purposes, the table also lists channels utilized by the aircraft-mounted Ocean Color Sensor (OCS) and Multi-Channel Ocean Color Scanner (MOCS) and the Nimbus 7 satellite-borne Coastal Zone Color Scanner (CZCS), all of which overflew the Nantucket Shoals experiment area. For direct solar measurements, a neutral density filter of optical density $\sim$4.0 is mounted on the barrel of the photometer. For this experiment, the filter remained in place for sky radiance measurements. For irradiance measurements (total or sky), an irradiance cap (cosine collector) designed by the Visibility Laboratory of the Scripps Institution of Oceanography was mounted in place of the neutral density filter.

Photometer Control Unit

The photometer control unit provides a high voltage power source for the PMT. Four fixed voltages are provided which allow gain settings to be selected at fixed intervals. A variable voltage control option is also provided. The unit displays LCD digital readouts of source and output photometer voltages, and PMT temperature. Under normal operations, the PMT temperature is maintained at about 10° C. A battery-powered LCD digital clock is provided for field use.

Solar Tracker Unit

The Research Support Instruments Solar Tracker System (Model 90-183) is an electromechanical device designed to actively point the solar photometer at the Sun, even from unstable platforms. The tracker maintains active control in two axes, designated pitch and roll. By a combination of these motions, the device can track the Sun anywhere in the upper hemisphere. A quadrant detector assembly with dual-stepper drive allows solar tracking to within 0.1° accuracy. Three modes of operation are possible: (1) manual mode allows the operator to point the instrument at any point in the sky, (2) sky-scan mode drives the tracker back and forth in a raster pattern sweeping arcs across the sky from horizon-to-horizon at 20° intervals, and (3) automatic tracking utilizes the quadrant detector to locate and maintain sight of the Sun. If the intensity measured falls below a threshold value, pitch and roll axes are commanded to search and regain a lock on the Sun. A 2.5-second system delay allows for momentary shadowing effects. The entire tracker was mounted for this experiment on a rotating turntable (see fig. 3) to allow azimuthal pointing.

Solar Tracker Controller

The control unit for the solar tracker includes all the controls for tracker operations and contains the microcomputer circuitry. A master control allows selection of the tracker mode of operation as described above. Two manually operated potentiometers allow control of the roll and pitch axes motions. A LED on the control panel indicates when the instrument locks on the Sun for tracking. For recording purposes, output consists of roll and pitch axes voltages, average quadrant detector signal, and locked tracking indication signal.

Data Recorder

The recorder used in this experiment was a Datel Systems, Inc. Data Logger (Model PPL-10A6) with a 10-channel input/output capability. In operation, the channels utilized provided photometer output voltage, filter wheel position (numbers 1 to 10 as voltages), roll and pitch voltages from the tracker unit as well as average quadrant detector output and locked tracking indication. The data logger requires a 1-second interval per channel of output. Frequency of output is controllable for automatic operation.

TEST PROCEDURES AND OPERATIONS

The solar photometer/tracker unit was set up in a parking area at Nantucket Airport, Nantucket Island on May 6, 1981. The controller units and recorder were stationed some distance away in a NASA vehicle. A true north line was determined to align the tracker unit. This established a reference system for the roll and pitch voltages output from the unit as shown in figure 3. Additionally, with true north established, the turntable containing the photometer/tracker assembly could be rotated to any azimuth heading to obtain scans in any vertical plane (with pitch angle set to 0^{o}, the photometer is rotated about the roll axis from horizon ($+90^{o}$) to horizon (-90^{o}) in that direction.

For this experiment, planned measurements fell into three categories: (1) atmospheric optical depths, (2) sky radiance over a range of scattering angles, and (3) irradiances from the total hemisphere (including the direct solar beam) and from skylight alone (with the direct solar beam obscured).

Optical Depth Measurements

To obtain data from which atmospheric optical depths could be calculated, the photometer, with neutral density filter attached, was pointed directly at the Sun by using the tracker unit in the automatic Sun-tracking mode. Photometer voltages in each of the 10 channels (see table 1) were recorded along with the channel (filter wheel) number and roll-pitch voltages from the tracker. The data frequency was determined by the solar elevation angle (measured horizon up)--every 15 minutes when the Sun was less than 30^{o} elevation and a half-hour frequency for higher solar elevations. The greater frequency is necessitated by large changes in air-mass values with changes in solar elevation angle (air mass is approximately given by the cosecant of the solar elevation angle).

Sky Radiance Measurements

To obtain sky radiance for a wide range of scattering angles, photometer measurements were made within the plane containing the Sun and local vertical, designated the Sun plane. This was accomplished by rotating the photometer/tracker unit until the pitch axis was aligned with the Sun azimuth, setting the pitch voltage for zero pitch angle, and rotating the photometer about the roll axis from horizon to horizon. As the data recorder required 1 second to output each variable, it was necessary to fix the photometer at a selected pointing roll angle, record the photometer voltages in each of 10 wavelengths plus filter wheel position and roll voltages, before manually rotating about the roll axis to a new pointing direction in the Sun plane. Up to half an hour was required for a complete horizon to horizon Sun plane scan because of the manual filter wheel changes and slow data-recording frequency. As the Sun's azimuth could change appreciably during a half-hour period, the tracker table was rotated as required to maintain a Sun-plane alignment.

A similar experimental procedure was used for scans in a vertical plane perpendicular to the Sun plane, henceforth referred to as the "normal plane scan." While the range of scattering angles which can be attained in a normal-plane scan is generally smaller than that for a Sun-plane scan, it provides a check on the homogeneity of the atmosphere as equal scattering angles to either side of the Sun plane should yield the same photometer readings.

All photometer data for Sun plane and normal plane scans were obtained with the neutral density filter in place. Because of the length of time required for such scans, a maximum of three were recorded on any one day.

Total and Sky Irradiance Measurements

For irradiance measurements, an irradiance cap was used in place of the neutral density filter on the photometer barrel. All irradiance data were measured with the photometer pointed vertically, i.e., 0° pitch and 0° roll (see fig. 3). Photometer voltage readings in each of 10 channels and filter wheel number were recorded corresponding to irradiance from the entire upper hemisphere including the direct solar beam (total irradiance). The irradiance cap was then shadowed using a cardboard disk obscuring the direct solar beam and photometer voltages corresponding to skylight irradiance only recorded. Irradiance measurements were generally taken at hour intervals. In some instances, skylight irradiance measurements were omitted due to time considerations.

Table 2 summarizes atmospheric data collection periods during the experiment. Generally, data were recorded during periods of clear skies which included May 7, 8, 9, 13, and 14. Efforts were made to include data taken at low solar elevation angles to ensure a significant range of air-mass values.

DATA ANALYSIS AND RESULTS

Relative solar-sensor geometry is essential information in analyzing measured atmospheric data. The solar elevation angle, θ_s, measured horizon up was determined by the relation

$$\sin \theta_s = \sin L \sin D + \cos L \cos D \cos h \tag{1}$$

where L is the local latitude, D the solar declination, and h the hour angle given by

$$h(\text{deg}) = 15(T - M) - L_o \tag{2}$$

where $T(\text{hr})$ is the time (GMT) of the measurement, $M(\text{hr})$ the time of meridian Sun passage (true solar noon), and $L_o(\text{deg})$ is the local longitude measured positive west from Greenwich. Complete details of these calculations including daily corrections for D and M are given in reference 1. For solar azimuth, A_s, the relation

$$\sin A_s = \sin h \cos D \sec \theta_s \tag{3}$$

was used (ref. 2) with A_s transformed by quadrants to range from 0° to 360° measured clockwise from true north.

The atmospheric air mass, m, is a measure of a slant path air mass, at pointing elevation angle θ, relative to the air mass at zenith. It is approximately given by

$$m(\theta) = \csc \theta \tag{4}$$

For greater accuracy, however, for angles $\theta > 10^{\circ}$ the relation

$$m(\theta) = \csc (\theta + 1.5\theta^{-0.72}) \tag{5}$$

was used as given by reference 3. For low elevation angles, $\theta < 10^{\circ}$, the tabular values of m given by reference 4 were used. Two types of air-mass values arose in the calculations: $m(\theta_s)$ represents air-mass values in the direction of the Sun (solar elevation angle θ_s given by eq. (1)) whereas $m(\theta_p)$ represent air-mass values in any photometer pointing direction (photometer pointing elevation angle, θ_p, determined from roll-pitch voltages of tracker). When the photometer points at the Sun, these air-mass values are identical.

The scattering angle, ϕ, is the direction of single-scattered solar radiation relative to its initial direction and is given by reference 5 as:

$$\cos \phi = \cos \theta_s \cos \theta_p \cos \alpha + \sin \theta_s \sin \theta_p \tag{6}$$

where θ_s is the solar elevation angle as before, θ_p is the pointing elevation angle of the photometer, and α is the azimuth of the photometer measured from the Sun plane. Forward scattered radiation is given by $0^{\circ} \leqq \phi \leqq 90^{\circ}$ whereas backscattered radiation occurs when $90^{\circ} \leqq \phi \leqq 180^{\circ}$.

As shown in table 2, the atmospheric data collected during the Nantucket Shoals experiment fell into three main categories including measurements for (1) optical depths, (2) sky radiance distributions, and (3) total and skylight irradiances. The analysis and results for each category are described separately below.

Optical Depth Analysis and Results

The solar photometer was calibrated, with neutral density filter attached, at the Visibility Laboratory of the Scripps Institution of Oceanography using a standard lamp irradiance source. Source radiance, $L_s(\lambda)$, was then related to measured photometer voltages, $V_p(\lambda)$, by

$$L_s(\lambda) = C(\lambda)V_p(\lambda) \tag{7}$$

where $C(\lambda)$ are calibration constants for the 10 wavelength bands, λ, used in the experiment (see table 1). The photometer was found, during the calibration process, to have a slight nonlinearity which could be accounted for by use of

$$L_s(\lambda) = C_s(\lambda)V_p(\lambda)^{1/a} \tag{8}$$

in place of equation (7). The power, a, was found by regression analysis to be 1.0174. The new calibration constants $C_s(\lambda)$ apply to the nonlinear model and were found by equating equations (7) and (8) at the calibration voltages.

To find optical depths, the voltages corresponding to the solar radiance at the top of the atmosphere, $L_o(\lambda)$, were computed and are referred to as the zero air-mass voltages, $V_o(\lambda)$. The values of $L_o(\lambda)$ were derived from the solar extraterrestrial irradiance values for the Sun given by reference 6. Total optical depths of the atmosphere, $\tau(\lambda)$, normalized to one air mass, are then given by

$$\tau(\lambda) = -\frac{\ln\left[V_p(\lambda)/V_o(\lambda)\right]^{1/a}}{m(\theta_s)} \tag{9}$$

Similar calculations are performed in references 7 and 8, for example.

During the interim period between May 9 and May 13, the neutral density filter used in the Scripps' calibration of the photometer suffered irreparable water damage. As a result, a replacement optical density 4.0 neutral density filter was used for all data taken on May 13 and 14. Experience with neutral density filters has shown wide variations in the optical density magnitudes. The calibration constants, $C_s(\lambda)$, and hence, zero air-mass voltages, $V_o(\lambda)$, used for the May 7-9 data could not be relied on as accurate for use for the May 13-14 data. Also, the transmission curve for the original neutral density filter was no longer available. Thus, a technique whereby the zero-air-mass voltages are corrected by a ratio of neutral density filter transmissions also could not be used.

As the data of May 13 and 14 were obtained with an uncalibrated instrument, the so-called Langley plot method (see refs. 5, 9, 10, and 11, for example) was used to estimate zero air-mass voltages corresponding to the changed photometer configuration. The technique basis is evident if equation (9) is rewritten as

$$\ln V_p(\lambda) = \ln V_o(\lambda) - \tau(\lambda)m(\theta_s)a \tag{10}$$

Plotting measured photometer voltates, $V_p(\lambda)$, on a natural log scale versus variable air-mass values, then the intercept value when the air mass goes to zero is the natural log of the zero air-mass voltage for that wavelength. An assumption is made that the total optical depth, $\tau(\lambda)$, remains constant over the observation period. May 14 was a favorable day for the use of the technique.

A total of 18 photometer observations of the Sun were taken between 0545 and 1200 hours EDT. The three earliest observations were dropped because they were measured through excessive slant path distances and the last three observations were dropped due to clouds building in the general area. The remaining 12 observations were used in a linear regression analysis of equation (10) for the time period 0630 to 1030 hours EDT over which the air-mass values ranged from 5.12 to 1.22. The correlation coefficients (R^2) for all wavelengths were greater than 0.978 indicating that the linear relationship in equation (10) is a very good representation of the data. Figure 4 shows the Langley plots for 3 of the 10 wavelengths--400, 550, and 750 nm. The zero air-mass voltages obtained by the Langley plot method for the data measured on May 13 and 14 are compared below to those values obtained from the measured data of May 7-9 made by using the calibrated photometer/neutral density filter system:

Wavelength (nm)	$V_o(\lambda)$ May 7-9 (volts)	$V_o(\lambda)$ May 13-14 (volts)
400	6.061	6.693
440	5.732	6.694
490	5.725	6.859
520	6.669	7.977
550	6.685	8.814
580	6.919	9.125
610	5.905	8.044
670	4.452	5.984
700	3.831	4.951
750	3.993	5.080

The observed increases in zero air-mass voltages for May 13 and 14 are consistent with the generally observed increased photometer voltages measured for May 13 and 14 compared to those measured during the May 7-9 period.

By using the total optical depths from equation (9) and the appropriate zero air-mass voltages, the unit air-mass transmittances, T, are given by

$$T(\lambda) = e^{-\tau(\lambda)} \tag{11}$$

The total optical depth can be written as the sum of optical depths due to Rayleigh or molecular scattering, $\tau_R(\lambda)$, ozone absorption, $\tau_{O_3}(\lambda)$, and aerosols, $\tau_A(\lambda)$ or,

$$\tau(\lambda) = \tau_R(\lambda) + \tau_{O_3}(\lambda) + \tau_A(\lambda) \tag{12}$$

Reference 12 discusses this relationship in detail. The Rayleigh optical depth can be computed by the method of reference 13 using

$$\tau_R(\lambda) = 0.00838\lambda^{-(3.916 + 0.074\lambda + 0.050/\lambda)} \tag{13}$$

where λ are in microns at the center wavelengths of the bands used. The ozone optical depth values, $\tau_{O_3}(\lambda)$, were supplied by Scripps Institution of Oceanography for the present instrument wavelength bands. Reference 12 presents a method of computing these values. Figure 5 shows both the Rayleigh and ozone optical depths for the range of wavelengths considered in this experiment.

Equation (12) can obviously be used to compute aerosol optical depths as

$$\tau_A(\lambda) = \tau(\lambda) - \tau_R(\lambda) - \tau_{O_3}(\lambda) \tag{14}$$

The field-of-view for the solar photometer was 10°. Since the Sun subtends an angle of about 0.5°, it is evident that a portion of the measured photometer voltage is due to forward scattered radiation from the aureole around the Sun. It is shown in reference 11, for example, that with a 3° field-of-view, the diffuse flux from the aureole contributes less than 2 percent of the total observed flux. Reference 14 presents a method whereby the aerosol optical depths can be adjusted by a factor $\overline{R}_p$ to account for the contribution from aureole flux. The factor is shown to depend on the field-of-view of the instrument (expressed as a half-cone angle) and an estimate of the exponent, ν, assuming a Junge distribution of aerosol particle sizes. A Junge distribution is given by

$$\psi(r) = Cr^{-(\nu^*+1)} \tag{15}$$

where $\psi(r)\,dr$ represents the number of particles per unit volume with radii between limits r and $r + dr$; C is a scaling constant, and ν^* is a shaping constant whose value normally lies in the range from 2 to 4. Reference 11 demonstrates a method whereby ν^* can be determined by a plot of $\ln\left[\tau_A(\lambda)\right]$ versus $\ln \lambda$. The slope of such a line is shown to be $(-\nu^* + 2)$. In practice, time-averaged values of $\tau_A(\lambda)$ were used for each of the experiment days and a linear regression analysis used to relate $\ln\left[\overline{\tau}_a(\lambda)\right]$ to $\ln \lambda$. It should be noted that the shaping constants of references 14 and 11 are related by

$$\nu = \nu^* + 1 \tag{16}$$

With ν and the field-of-view known (half-cone angle = 5°), the aerosol correction factors $\overline{R}_p$ were obtained on a day-by-day basis using reference 14.

The Junge distribution shaping factor, ν^*, and aerosol correction factor, $\overline{R}_p$, are summarized below:

Date	ν^*	$\overline{R}_p$
May 7	4.365	0.982
May 8	3.319	0.964
May 9	3.380	0.968
May 13	2.693	0.920
May 14	3.479	0.972

The aerosol optical depth corrections range from 2 percent to 8 percent depending on the day. The corrected aerosol optical depths, $\tau_{A,C}(\lambda)$, are given by

$$\tau_{A,C}(\lambda) = \frac{\tau_A(\lambda)}{\overline{R}_p} \qquad (17)$$

and corrected total optical depths are given by

$$\tau_C(\lambda) = \tau_R(\lambda) + \tau_{O_3}(\lambda) + \tau_{A,C}(\lambda) \qquad (18)$$

The preceding analysis was performed (as a function of time and wavelength) on the five data sets described in table 2, and yielded tables of instantaneous (corrected) total optical depths, total transmittances, and aerosol optical depths. Average values were calculated, avoiding very low Sun angles or noted cloudy times, of total optical depths, total transmittances, aerosol optical depths, and their standard deviations versus wavelength. Rayleigh and ozone optical depths were included for completeness. The results are presented on a daily basis for May 7-9 and May 13-14 as tables 3 to 7.

Figure 6 summarizes the observed average aerosol optical depths for the 5 experiment days. Except for May 13, for which little usable data were available due to cloud buildup, the spectral shapes of the curves are similar, but differ considerably with regard to optical depth magnitude. May 7 represented, on average, the optically clearest period (highest transmittances) whereas May 14 represented, on average, the least optically clear period (lowest transmittances).

For each day, the total instantaneous optical depth histories for wavelengths 400, 550, and 750 nm were plotted as figures 7(a) to 7(e) to examine atmospheric stability. Hourly optical depth variations are easily verified from these figures. On May 7 (fig. 7(a)), the optical depth decreased with time at 400 nm but increased at 750 nm. On May 9 (fig. 7(c)), the optical depths at both 400 and 750 nm increased. The large variations on May 13 (fig. 7(d)) are due to clouds, whereas the low optical depth readings obtained at the three earliest times on May 14 (fig. 7(e)) are due to low Sun angle effects. May 8 (fig. 7(b)) demonstrated a higher frequency "noise" level than that observed for May 9 (fig. 7(c)).

Sky Radiance Analysis and Results

The solar photometer was calibrated by Scripps Institution of Oceanography for sky radiance measurements by pointing the instrument (without neutral density filter) at a barium sulfate 100 percent diffuse white reflector plate illuminated by a standard lamp source. In a manner similar to the Sun calibration, a non-linear model can be used to relate observed radiances to measured voltages to obtain calibration constants. Unfortunately, the sky radiance measurements performed at the test site during the period May 7-14 were made with 4.0 neutral density filters in place. Under such circumstances, the laboratory calibrations could not be used to calculate absolute radiance values. To recover some information from the recorded data, the decision was made to present the radiance information obtained in a normalized form as a function of scattering angle.

As noted in table 2, the available sky radiance data were measured during Sun-plane and normal-plane scans with the photometer. The scattering angles are given by equation (6) where θ_s are the solar elevation angles during the observation periods and θ_p are the instrument pointing angles given by the calibration equation

$$\theta_p(\text{deg}) = 329.56 - 53.39V_R \qquad (19)$$

with V_R the tracker unit roll voltages. The angle α in equation (6) for Sun-plane scans is 0^o toward the Sun side and 180^o away from the Sun side, whereas for normal-plane scans, it assumes values of 90^o or -90^o on either side of the Sun plane (plane of assumed symmetry).

Equation (7) can be rewritten as

$$\frac{L_{sky}(\phi,\lambda)}{C_{sky}(\lambda)} = V_p(\phi,\lambda)^{1/a} \qquad (20)$$

where the photometer voltages $V_p(\phi,\lambda)$ now are proportional to the sky radiances, $L_{sky}(\phi,\lambda)$. The constants of proportionality, $C_{sky}(\lambda)$ are unknown.

Air-mass values, $m(\theta_p)$, corresponding to the photometer pointing elevation angles vary considerably during plane scans. Assuming scattering is symmetrical, even at the same scattering angle the sky radiances can vary considerably due to the variable slant paths (i.e., variable air-mass values). A technique developed in reference 15 and employed in references 5 and 10 corrects for this air-mass effect by normalizing all radiances to a unit air mass:

$$\bar{L}_{sky}(\phi,\lambda) = L_{sky}(\phi,\lambda) \left\{ \frac{(1 - T)}{\left[1 - T^{m(\theta_p)}\right]} \right\} \tag{21}$$

where $\bar{L}_{sky}(\phi,\lambda)$ are now sky radiances independent of the air-mass effect and T are the total transmittance values at the time of observations. Combining equations (20) and (21) yields

$$L'(\phi,\lambda) = \frac{\bar{L}_{sky}(\phi,\lambda)}{C_{sky}(\lambda)} = V_p(\phi,\lambda)^{1/a} \left\{ \frac{(1 - T)}{\left[1 - T^{m(\theta_p)}\right]} \right\} \tag{22}$$

Finally, if the above equation is normalized to the sky radiance for some scattering angle, say $\phi = 45^o$, then the calibration constants disappear:

$$\frac{L'(\phi,\lambda)}{L'(45^o,\lambda)} = \frac{\bar{L}_{sky}(\phi,\lambda)}{\bar{L}_{sky}(45^o,\lambda)} = \frac{V_p(\phi,\lambda)^{1/a} \left\{ \frac{(1 - T)}{\left[1 - T^{m(\theta_p)}\right]} \right\}}{L'(45^o,\lambda)} \tag{23}$$

In practice, $L'(\phi,\lambda)$ are calculated from equation (22) for all ϕ using transmittance values obtained from the optical depth analysis. A power-law regression analysis is used on the $L'(\phi,\lambda)$ versus ϕ distribution to obtain the normalization factors $L'(45^o,\lambda)$. Ratios formed by equation (23) represent normalized sky radiance distributions versus scattering angle. The same procedure applies to data obtained from Sun-plane and normal-plane scans. Tables 8 to 12 present the results of this analysis. Listed are the types of scan and date, the times of observation and corresponding solar elevation angles, the air-mass values corresponding to the specific photometer pointing elevation angles (not listed), and the resulting scattering angles corresponding to horizon-to-horizon sweeps by the photometer. Finally, the instantaneous normalized sky radiances are listed as functions of both wavelength and phase angle. Figures 8(a) to 8(d) present the results for several Sun-plane and normal-plane scans at 400 nm and 750 nm wavelengths. Open and solid circle symbols distinguish scattering angles obtained on opposite sides of the Sun for Sun-plane scans ($\alpha = 0^o$ or 180^o, see eq.(6)) or for normal-plane scans to either side of the Sun plane ($\alpha = 90^o$ or -90^o). The May 7 Sun-plane scan demonstrates the expected pattern of marked forward scattering at small scattering angles and a rapid decrease towards the high scattering angles. The normal-plane scan of May 7 displays a distinct asymmetric behavior according to which side of the Sun plane the scan occurs. Since the air-mass effect has been accounted for, the asymmetry may be tied to an inhomogeneity of the atmosphere.

In marked contrast is the normal plane scan of May 13 which is highly symmetric with respect to the Sun plane.

It was observed that for fixed wavelengths, the normalized radiance functions for different times or days were very similar in shape at least up to the maximum observed scattering angles measured ($\sim 130^{\circ}$). Figure 9 illustrates this effect for the three Sun-plane scans of May 8 at two wavelengths. Reference 16 demonstrates the variation in phase functions depending on visibility and geographic location. Significant shaping variations for backscattered radiation ($\phi > 90^{\circ}$) are presented. Therefore, it cannot be concluded that the behavior shown in figure 9 applies beyond the scattering angles considered.

For a satellite-borne remote sensor being used to observe oceanographic phenomena, sunlight scattered back towards the sensor without having reached the surface, path radiance, constitutes a significant percentage of the total observed signal by a remote sensor, such as a satellite. By matching single-scattering angles of radiation scattered toward the remote sensor and that scattered toward the ground-based instrument, the ground-based sky radiance measurements become an estimate of path radiance observed by the sensor. Data such as just presented, in an absolute format, constitute the basis of such an approximation. References 10 and 17 describe the technique and introduce an additional correction factor to account for a remote sensor overflight time not coincident with the time of the measured sky radiance distribution.

Irradiance Analysis and Results

An irradiance cap for the solar photometer was unavailable during the Scripps Institution of Oceanography's calibration of the instrument. As a result, no irradiance calibrations were available for reducing total and sky irradiance voltage data as measured by the instrument during the Nantucket Shoals experiment. An alternative technique for on-site calibration was adopted which appears to give good results in deriving absolute total and sky irradiances.

As shown in reference 5, the total irradiance, H, measured by a ground-based sensor can be considered as a sum of the attenuated direct solar irradiance and a diffuse sky irradiance, H_{sky}:

$$H(\lambda) = H_o(\lambda)T(\lambda)^{m(\theta_s)} \sin \theta_s + H_{sky}(\lambda) \tag{24}$$

where $H_o(\lambda)$ are solar irradiance values outside the atmosphere for the experiment day (see ref. 6), $m(\theta_s)$ are the air-mass values corresponding to the solar elevation angles, θ_s, during the observation period, and the transmittances, T, are interpolated from previously calculated values listed in tables 3 to 7.

During the May 7-14 experiment period, photometer voltages were obtained which corresponded to total and sky irradiances. The voltages measured with an unshaded irradiance cap, $V_{p,tot}(\lambda)$, represented total irradiances whereas when the irradiance cap was shadowed, and the direct solar beam obscured, the voltages, $V_{p,sky}(\lambda)$, represented sky irradiances. Assuming a nonlinear proportionality between irradiances and voltages, then:

$$H(\lambda) = K(\lambda)V_{p,tot}^{1/a}(\lambda) \qquad (25a)$$

$$H_{sky} = K(\lambda)V_{p,sky}^{1/a}(\lambda) \qquad (25b)$$

The proportionality constants, $K(\lambda)$, represent the required calibration constants. Substitution of equations (25a) and (25b) into equation (24) yields a solution for the calibration constants:

$$K(\lambda) = \left[\frac{H_o(\lambda)T(\lambda)^{m(\theta_s)} \sin \theta_s}{V_{p,tot}^{1/a} - V_{p,sky}^{1/a}}\right]^a \qquad (26)$$

All variables in equation (26) are known from previous measurements and derivations. Ideally, $K(\lambda)$ will be invariant during the experiment period. However, variations will result from uncertainties in the measured or derived terms as well as the accuracy with which the direct solar beam is obscured. To overcome this uncertainty, 10 sets of total and sky irradiance voltages were used at each wavelength to calculate a set of average calibration constants, $K(\lambda)$. Performing the calculations, it was found that the coefficients of variation, the ratio expressed as a percentage of standard deviation to mean values, ranged from 3.7 to 6.2 percent depending on the wavelengths. These low dispersion values demonstrate the nearly constant behavior of $K(\lambda)$ over significant time variations. As a result, the average calibration constants, $K(\lambda)$, were judged acceptable for use in equations (25a) and (25b).

After the experiment, a construction flaw was discovered in the irradiance cap which caused it to deviate from a perfect cosine collector for elevation angles below 30^o. For this reason, no data for solar elevation angles below 30^o are reported which would present the greatest errors in total irradiance. An indeterminate degree of error is present for all diffuse irradiance collected from portions of the sky below 30^o elevation.

With the above considerations in mind, equations (25a) and (25b) were used with derived calibration constants to calculate total and sky irradiances. These results, along with the ratio of sky to total irradiance, are presented as tables 13 to 15 for the 5 experiment days. In some instances, sky irradiance measurements were not taken due to time considerations. The general observations that the proportion of sky irradiance to total irradiance increases with decreasing wavelength or solar elevation angle is easily confirmed by the tabulated results.

RECOMMENDATIONS

As this was the first use of this photometer system in a field test, some equipment and operational deficiencies are to be expected. Recommendations for overcoming these deficiencies and improving the operational aspects of future experiments are given below.

Calibration Recommendations

Laboratory calibrations of the solar photometer should be performed for all categories of measurements (optical depths, sky radiance, and irradiance measurements) including extra calibrations using spare neutral density filters. All field measurements should be made with the instrument configured as calibrated in the laboratory. Consideration should be given to calibrations using the Langley plot method for periods of good atmospheric stability such as found at high mountain elevations. The on-site irradiance calibration technique discussed in this report should be compared with laboratory calibrations in future experiments.

Equipment Recommendations

The field of view of the instrument should be reduced to 3^{o} or less and the photometer calibrated in this configuration to reduce the diffuse solar aureole contributions during optical depth measurements and integrating effects on the sky radiance measurements. A tape recording system should replace the digital data logger unit to simultaneously record multiple-wavelength photometer and solar tracker voltages. This would considerably reduce the time required for planar scans. Also, consideration should be given to automatic or remote operation of the filter wheel for channel selection.

Experiment Recommendations

Planar scans should be performed at low solar elevation angles to extend sky radiance distributions further into the backscattered region ($90^{o} < \phi \leq 180^{o}$). Also, consideration should be given to modify the tracker unit to scan in almucantar-type motions, i.e., circular, fixed-altitude sky scans about the local zenith, representing constant air mass but variable scattering angles.

CONCLUDING REMARKS

Ground-based atmospheric optical data were obtained during a Nantucket Shoals oceanographic experiment conducted during the period May 7-14, 1981.

Analysis of these data has yielded total and aerosol optical depths, transmittances, normalized sky radiance distributions, and total and sky irradiances. Problems in instrument calibration and operational procedures precluded the measurement of absolute sky radiances, and the total and sky irradiances were derived using a post-experiment calibration technique. The results of this analysis may aid in atmospheric correction of remote sensor data obtained by several sensors overflying the Nantucket Shoals area. Recommendations concerning future experiments using the described solar photometer system have centered on calibration and operational deficiencies uncovered during this experiment.

REFERENCES

1. Woolf, Harold M.: On the Computation of Solar Elevation Angles and the Determination of Sunrise and Sunset Times. NASA TMX-1646, September 1968.

2. Bowditch, N.: American Practical Navigator. U.S. Naval Oceanographic Office, H. O. Pub. No. 9, Washington, D.C., 1966, U.S. Government Printing Office.

3. Nagel, M. R.: Improved Approximation of Bemporad's Airmass Function. Applied Optics, vol. 13, no. 5, May 1974, pp. 1008-1009.

4. Kondrat'ev, K. Ya.: Radiation Characteristics of the Atmosphere and the Earth's Surface. NASA TTF-678, 1973.

5. Rogers, Robert H.; and Peacock, Keith: A Technique for Correcting ERTS Data for Solar and Atmospheric Effects. NASA SP-327, 1973.

6. Thekaekara, M. P.: Extraterrestrial Solar Spectrum, 3000-6100 Å at 1-Å Intervals. Applied Optics, vol. 13, no. 3, March 1974, pp. 518-522.

7. Wilson, Wayne H.: Measurements of Atmospheric Transmittance in a Maritime Environment. SPIE, vol. 195, August 1979, pp. 153-159.

8. Yulong, X.; Limin, Z.; Yonghau, Z.; and Shufang, Y.: The Influence of the Atmosphere on Remote Sensing in South-West China. Fourteenth International Symposium on Remote Sensing of Environment (Ann Arbor, Michigan), April 1980.

9. Slater, Philip N.: Remote Sensing - Optics and Optical Systems. Addison-Wesley Publishing Co., 1980.

10. Sturm, B.: Determination of Beam Transmittance and Path Radiance in the Four Bands of the ERTS-Satellite. Proceedings of DFVLR-Seminar on Remote Sensing, April 7-11, 1975, at Porz-Wahn (Germany).

11. Shaw, Glenn E.; Reagan, John A.; and Herman, Benjamin M.: Investigations of Atmospheric Extinction Using Direct Solar Radiation Measurements Made with a Multiple Wavelength Radiometer. J. Applied Meteorology, vol. 12, March 1973, pp. 374-380.

12. Turner, Robert E.: Atmospheric Transformation of Multispectral Remote Sensor Data. NASA CR-135338, 1977.

13. Frohlich, C.; and Shaw, Glenn E.: New Determination of Rayleigh Scattering in the Terrestrial Atmosphere. Applied Optics, vol. 19, no. 11, June 1980, pp. 1773-1775.

14. Box, M. A.; and Deepak, A.: Atmospheric Scattering Corrections to Solar Radiometry. Applied Optics, vol. 18, no. 12, June 1979, pp. 1941-1949.

15. Gordon, Jacqueline I.; Harris, James L.; and Duntley, Siebert Q.: Measuring Earth-to-Space Contrast Transmittance From Ground Stations. Applied Optics, vol. 12, no. 6, June 1973, pp. 1317-1324.

16. Barteneva, O. D.: Scattering Functions of Light in the Atmospheric Boundary Layer. Izv. Geophys. Ser., 1960, pp. 1852-1865.

17. Peacock, Keith: Ground-Based Determination of Atmospheric Radiance for Correction of ERTS-1 Data. Applied Optics, vol. 13, no. 12, December 1974, pp. 2741-2742.

TABLE 1.- SOLAR PHOTOMETER OPTICAL FILTERS

Filter number	Center wavelength (nm)	Bandwidth* (nm)	Transmission (percent)
1	400	10.1	50
2	440	7.4	48
3	490	7.1	52
4	520	8.0	58
5	550	9.1	46
6	580	9.0	62
7	610	9.9	54
8	670	11.2	55
9	700	13.0	49
10	750	14.0	57

*Half-maximum.

Center Wavelengths (nm) of Other Sensors

Ocean Color Sensor (OCS)	Multi-channel Ocean Color Scanner (MOCS)	Nimbus 7 Coastal Zone Color Scanner (CZCS)
428		
466		433
508	400 to 700 nm	520
549	20 channels	550
592	Each 15 nm wide	670
632		750
674		
714		
756		
794		

TABLE 2.- ATMOSPHERIC DATA COLLECTION PERIODS

Date	Optical depth measurements, start-stop time EDT	Sun-plane scans, start-stop time EDT	Normal-plane scans, start-stop time EDT	Irradiance measurements, start-stop time EDT
May 7	1130-1742	1335-1400	1240-1305	1150-1554
May 8	0650-1800	(1) 0945-1025 (2) 1315-1350 (3) 1556-1627	---	0910-1547
May 9	0620-1058	---	---	0906-1105
May 13	1319-1601	---	1229-1305	1530
May 14	0545-1200	(1) 0910-0930 (2) 1213-1226	0812-0830	0905-1204

Table 3.- Atmospheric optical properties for May 7, 1981.

Time EDT	Solar Alt. (deg)	Total optical depths for specified wavelengths (nm). 400	440	490	520	550	580	610	670	700	750
1130	61.7	.596	.431	.308	.272	.176	.183	.171	.070	.082	.095
1200	64.4	.591	.398	.275	.256	.167	.177	.168	.098	.104	.094
1230	65.6	.594	.412	.279	.253	.167	.177	.173	.091	.096	.103
1307	64.8	.585	.426	.297	.267	.178	.182	.171	.101	.101	.098
1411	58.4	.576	.415	.298	.263	.184	.182	.173	.096	.097	.098
1430	55.6	.557	.427	.302	.266	.156	.177	.158	.088	.087	.099
1505	50.0	.568	.415	.298	.260	.190	.196	.164	.100	.103	.095
1535	44.8	.568	.423	.301	.266	.194	.203	.179	.118	.109	.105
1558	40.7	.567	.414	.301	.266	.200	.198	.181	.118	.115	.102
1633	34.2	.566	.421	.307	.277	.212	.218	.192	.129	.132	.114
1705	28.2	.551	.407	.297	.264	.211	.215	.190	.141	.122	.109
1742	21.3	.548	.411	.302	.268	.222	.221	.198	.131	.131	.113

Time EDT	Solar Alt (deg)	Total transmittances for specified wavelengths (nm). 400	440	490	520	550	580	610	670	700	750
1130	61.7	.551	.650	.735	.762	.839	.833	.843	.932	.921	.909
1200	64.4	.554	.671	.759	.774	.846	.838	.846	.907	.901	.910
1230	65.6	.552	.662	.757	.777	.846	.838	.841	.913	.908	.902
1307	64.8	.557	.653	.743	.766	.837	.834	.843	.904	.904	.906
1411	58.4	.562	.660	.742	.769	.832	.833	.841	.908	.908	.907
1430	55.6	.573	.652	.740	.766	.856	.837	.854	.916	.916	.906
1505	50.0	.566	.661	.742	.771	.827	.822	.848	.905	.903	.909
1535	44.8	.567	.655	.740	.767	.824	.817	.836	.888	.897	.900
1558	40.7	.567	.661	.740	.767	.818	.820	.834	.889	.891	.903
1633	34.2	.568	.656	.735	.758	.809	.804	.825	.879	.876	.892
1705	28.2	.576	.666	.743	.768	.810	.806	.827	.868	.885	.896
1742	21.3	.578	.663	.740	.765	.801	.802	.820	.878	.877	.893

Table 3.- Concluded.

Time EDT	Solar Alt (deg)	Aerosol optical depths at specified wavelengths (nm). 400	440	490	520	550	580	610	670	700	750
1130	61.7	.233	.184	.142	.131	.052	.069	.071	.009	.017	.056
1200	64.4	.228	.151	.109	.116	.043	.063	.068	.037	039	.055
1230	65.6	.232	.165	.113	.112	.043	.063	.073	.030	.031	.065
1307	64.8	.223	.179	.131	.127	.054	.068	.071	.040	.035	.059
1411	58.4	.214	.168	132	.123	.059	.069	.074	.035	.031	.059
1430	55.6	.195	.180	.136	.126	.032	.063	.058	.027	.022	.060
1505	50.0	.206	.167	.132	.119	.066	.082	.065	.039	.037	.056
1535	44.8	.206	.175	.135	.125	.070	.089	.079	.057	.044	.066
1558	40.7	.205	.167	.134	.125	.076	.084	.081	.056	.049	.063
1633	34.2	.204	.174	.141	.136	.087	.104	.092	.068	.067	.075
1705	28.2	.189	.160	.131	.124	.086	.101	.090	.080	.056	.071
1742	21.3	.186	.164	.136	.127	.098	.107	.099	.069	.065	.074

WAVE LENGTH (NM)	AVG OPT DEPTH	RAY OPT DEP	OZONE OPT DEP	AERO OPT DEP	STD DEV OPD	AVG TOT TRANS	STD DEV TRANS
400	.568	.349	.013	.206	.014	.567	.008
440	.417	.235	.012	.170	.006	659	.004
490	.298	.151	.015	.132	.007	.742	.005
520	.265	.118	.022	.124	.006	.767	.004
550	.191	.094	.030	.067	.020	.826	.016
580	.197	.076	.038	.083	.016	.821	.013
610	.178	.062	.038	.078	.012	.837	.010
670	.111	.042	.019	.050	.018	.895	.016
700	.109	.035	.030	.044	.014	.897	.013
750	.104	.027	.012	.065	.006	.902	.006

Table 4.- Atmospheric optical properties for May 8, 1981.

Time EDT	Solar Alt (deg)	Total optical depths at specified wavelengths (nm). 400	440	490	520	550	580	610	670	700	750
650	13.7	.707	.548	.414	.370	.321	.313	.282	.215	.210	.181
717	18.7	.658	.510	.390	.357	.309	.308	.279	.212	.208	.181
733	21.7	.676	.528	.407	.374	.321	.316	.291	.223	.220	.197
746	24.1	.686	.536	.408	.377	.322	.321	.297	.219	.220	.198
802	27.1	.673	.526	.404	.375	.315	.316	.291	.220	.217	.192
839	34.0	.707	.553	.419	.388	.319	.319	.295	.219	.221	.200
859	37.8	.728	.574	.433	.395	.322	.328	.312	.234	.231	.205
936	44.5	.734	.556	.440	.409	.331	.333	.317	.235	.231	.224
1003	49.2	.709	.558	.419	.387	.296	.303	.284	.212	.213	.203
1100	58.2	.730	.570	.439	.398	.314	.319	.305	.226	.220	.213
1205	65.0	.734	.553	.417	.372	.289	.283	.282	.205	.223	.242
1230	65.9	.723	.550	.415	.389	.288	.281	.275	.197	.206	.193
1301	65.4	.717	.555	.429	.389	.297	.295	.288	.209	.210	.205
1406	59.2	.722	.565	.424	.392	.291	.299	.288	.197	.207	.200
1428	56.1	.716	.561	.417	.389	.300	.304	.283	.204	.210	.196
1540	44.1	.737	.577	.435	.407	.319	.324	.309	.227	.223	.211
1630	34.9	.759	.593	.458	.425	.350	.350	.408	.165	.241	.224
1700	29.3	.730	.574	.438	.406	.340	.341	.312	.236	.226	.208
1741	21.6	1.294	1.143	1.014	.982	.929	.925	.895	.821	.814	.791
1800	18.0	.702	.554	.413	.372	.332	.336	.315	.251	.251	.226

Table 4.- Continued.

Time EDT	Solar Alt (deg)	Total transmittances for specified wavelengths (nm). 400	440	490	520	550	580	610	670	700	750
650	13.7	.493	.578	.661	.691	.726	.731	.754	.807	.810	.834
717	18.7	.518	.601	.677	.700	.734	.735	.757	.809	.813	.834
733	21.7	.509	.590	.666	.688	.725	.729	.747	.800	.802	.821
746	24.1	.503	.585	.665	.686	.725	.725	.743	.803	.803	.821
802	27.1	.510	.591	.668	.687	.730	.729	.748	.803	.805	.825
839	34.0	.493	.575	.657	.678	.727	.727	.745	.803	.802	.819
859	37.8	.483	.563	.649	.674	.725	.720	.732	.791	.794	.815
936	44.5	.480	.574	.644	.664	.718	.716	.728	.791	.794	.800
1003	49.2	.492	.573	.658	.679	.743	.739	.753	.809	.808	.816
1100	58.2	.482	.566	.645	.671	.731	.727	.737	.798	.803	.808
1205	65.0	.480	.575	.659	.689	.749	.753	.755	.815	.800	.785
1230	65.9	.485	.577	.660	.678	.749	.755	.760	.821	.814	.824
1301	65.4	.488	.574	.651	.678	.743	.745	.750	.811	.810	.814
1406	59.2	.486	.569	.654	.676	.748	.742	.750	.821	.813	.819
1428	56.1	.489	.571	.659	.678	.741	.738	.753	.815	.810	.822
1540	44.1	.479	.561	.647	.666	.727	.723	.734	.797	.800	.810
1630	34.9	.468	.552	.633	.653	.704	.705	.665	.848	.786	.800
1700	29.3	.482	.563	.646	.667	.712	.711	.732	.790	.797	.812
1741	21.6	.274	.319	.363	.375	.395	.396	.409	.440	.443	.453
1800	18.0	.496	.574	.662	.689	.717	.715	.730	.778	.778	.798

Table 4.- Concluded.

Time EDT	Solar Alt (deg)	Aerosol optical depths at specified wavelengths (nm). 400	440	490	520	550	580	610	670	700	750
650	13.7	.345	.301	.248	.229	.196	.199	.182	.153	.145	.143
717	18.7	.295	.262	.224	.217	.185	.194	.179	.150	.142	.143
733	21.7	.314	.281	.241	.233	.197	.202	.192	.162	.155	.158
746	24.1	.324	.289	.242	.236	.197	.207	.197	.158	.154	.159
802	27.1	.310	.279	.238	.235	.190	.202	.191	.159	.152	.154
839	34.0	.345	.306	.253	.248	.195	.205	.195	.158	.156	.161
859	37.8	.366	.327	.267	.255	.198	.214	.212	.173	.166	.166
936	44.5	.372	.308	.274	.268	.207	.220	.217	.173	.166	.185
1003	49.2	.347	.310	.253	.246	.172	.189	.184	.151	.147	.164
1100	58.2	.368	.322	.273	.258	.190	.205	.205	.164	.154	.175
1205	65.0	.372	.305	.250	.232	.165	.170	.182	.143	.158	.203
1230	65.9	.361	.303	.249	.248	.164	.167	.175	.136	.141	.155
1301	65.4	.355	.308	.262	.248	.172	.181	.188	.148	.145	.167
1406	59.2	.360	.317	.258	.251	.167	.185	.188	.136	.142	.161
1428	56.1	.354	.313	.251	.248	.176	.190	.183	.143	.145	.157
1540	44.1	.374	.330	.269	.267	.195	.210	.209	.166	.158	.172
1630	34.9	.397	.346	.292	.285	.226	.236	.308	.104	.175	.185
1700	29.3	.367	.327	.271	.265	.215	.227	.212	.175	.161	.169
1741	21.6	.931	.896	.848	.841	.805	.811	.795	.760	.749	.752
1800	18.0	.340	.307	.247	.232	.208	.222	.215	.190	.186	.187

WAVE LENGTH (NM)	AVG OPT DEPTH	RAY OPT DEP	OZONE OPT DEP	AERO OPT DEP	STD DEV OPD	AVG TOT TRANS	STD DEV TRANS
400	.705	.349	.013	.343	.025	.494	.013
440	.547	.235	.012	.299	.018	.579	.010
490	.417	.151	.015	.251	.014	.659	.009
520	.383	.118	.022	.242	.014	.682	.009
550	.312	.094	.030	.188	.013	.732	.010
580	.312	.076	.038	.198	.015	.732	.011
610	.292	.062	.038	.193	.013	.747	.010
670	.218	.042	.019	.157	.011	.804	.009
700	.218	.035	.030	.153	.008	.804	.006
750	.203	.027	.012	.164	.016	.817	.013

Table 5.- Atmospheric optical properties for May 9, 1981.

Time EDT	Solar Alt (deg)	Total optical depths at specified wavelengths (nm). 400	440	490	520	550	580	610	670	700	750
620	8.4	.601	.459	.343	.309	.264	.262	.231	.171	.163	.137
629	10.0	.598	.458	.346	.312	.274	.272	.241	.175	.168	.144
655	14.8	.614	.470	.354	.318	.274	.274	.246	.178	.172	.149
716	18.7	.621	.481	.364	.332	.279	.281	.255	.187	.184	.161
731	21.5	.626	.481	.364	.333	.282	.284	.260	.189	.187	.166
746	24.3	.634	.490	.373	.338	.285	.287	.261	.192	.188	.168
800	26.9	.635	.493	.373	.339	.282	.285	.261	.192	.192	.174
840	34.4	.653	.500	.378	.350	.279	.283	.264	.194	.191	.175
900	38.1	.660	.510	.385	.355	.282	.288	.270	.197	.195	.183
930	43.6	.666	.510	.386	.359	.276	.269	.259	.187	.192	.182
959	48.7	.670	.521	.387	.362	.279	.280	.270	.193	.194	.182
1028	53.6	.683	.531	.395	.368	.272	.281	.272	.199	.182	.171
1058	58.1	.691	.534	.396	.368	.266	.279	.273	.192	.199	.183

Time EDT	Solar Alt (deg)	Total transmittances at specified wavelengths (nm). 400	440	490	520	550	580	610	670	700	750
620	8.4	.548	.632	.709	.734	.768	.769	.794	.843	.850	.872
629	10.0	.550	.633	.708	.732	.760	.762	.786	.839	.845	.866
655	14.8	.541	.625	.702	.728	.760	.761	.782	.837	.842	.862
716	18.7	.537	.618	.695	.718	.757	.755	.775	.830	.832	.851
731	21.5	.535	.618	.695	.717	.754	.753	.771	.828	.830	.847
746	24.3	.531	.613	.689	.713	.752	.750	.770	.825	.828	.845
800	26.9	.530	.611	.689	.713	.754	.752	.770	.825	.825	.841
840	34.4	.520	.607	.685	.705	.756	.753	.768	.823	.826	.839
900	38.1	.517	.601	.680	.701	.754	.750	.763	.821	.823	.833
930	43.6	.514	.601	.680	.699	.759	.764	.772	.829	.825	.834
959	48.7	.512	.594	.679	.696	.756	.756	.763	.825	.823	.834
1028	53.6	.505	.588	.674	.692	.762	.755	.762	.820	.834	.843
1058	58.1	.501	.586	.673	.692	.766	.756	.761	.825	.819	.833

Table 5.- Concluded.

Time EDT	Solar Alt (deg)	Aerosol optical depths at specified wavelengths (nm). 400	440	490	520	550	580	610	670	700	750
620	8.4	.239	.212	.177	.169	.140	.148	.131	.109	.097	.098
629	10.0	.235	.211	.179	.172	.150	.158	.141	.114	.103	.105
655	14.8	.251	.223	.188	.177	.150	.160	.146	.117	.107	.110
716	18.7	.259	.234	.198	.191	.155	.167	.155	.126	.118	.122
731	21.5	.264	.234	.198	.192	.158	.170	.160	.128	.121	.127
746	24.3	.272	.243	.207	.197	.161	.173	.162	.131	.123	.130
800	26.9	.273	.246	.207	.198	.158	.172	.162	.131	.127	.135
840	34.4	.291	.252	.212	.210	.155	.169	.164	.133	.126	.136
900	38.1	.298	.263	.219	.214	.158	.174	.170	.136	.130	.144
930	43.6	.303	.263	.220	.218	.152	.155	.159	.126	.127	.143
959	48.7	.308	.274	.221	.222	.155	.166	.171	.131	.129	.143
1028	53.6	.321	.284	.229	.227	.147	.167	.172	.137	.117	.132
1058	58.1	.329	.287	.230	.228	.142	.165	.174	.131	.134	.144

WAVE LENGTH (NM)	AVG OPT DEPTH	RAY OPT DEP	OZONE OPT DEP	AERO OPT DEP	STD DEV OPD	AVG TOT TRANS	STD DEV TRANS
400	.646	.349	.013	.284	.028	.524	.015
440	.498	.235	.012	.251	.023	.608	.014
490	.375	.151	.015	.209	.015	.687	.011
520	.344	.118	.022	.204	.018	.709	.013
550	.278	.094	.030	.153	.005	.758	.004
580	.280	.076	.038	.166	.006	.756	.004
610	.261	.062	.038	.161	.010	.770	.007
670	.190	.042	.019	.128	.007	.827	.006
700	.187	.035	.030	.122	.009	.829	.007
750	.170	.027	.012	.131	.012	.844	.011

Table 6.- Atmospheric optical properties for May 13, 1981.

Total optical depths at specified wavelengths (nm).

Time EDT	Solar Alt (deg)	400	440	490	520	550	580	610	670	700	750
1319	65.5	.606	.483	.362	.308	.299	.282	.296	.185	.158	.118
1330	64.5	.607	.489	.365	.314	.299	.291	.291	.188	.163	.117
1403	60.7	.626	.502	.372	.313	.300	.298	.298	.188	.165	.127
1431	56.6	.769	.631	.524	.457	.469	.489	.526	.452	.549	.509
1526	47.4	.684	.553	.413	.357	.336	.319	.313	.210	.184	.137
1601	41.1	1.296	1.176	1.057	.985	.977	.986	.934	.840	.754	.747

Total transmittances at specified wavelengths (nm).

Time EDT	Solar Alt (deg)	400	440	490	520	550	580	610	670	700	750
1319	65.5	.546	.617	.697	.735	.741	.754	.744	.831	.854	.888
1330	64.5	.545	.613	.695	.730	.742	.748	.748	.829	.850	.890
1403	60.7	.535	.605	.690	.731	.741	.742	.743	.829	.848	.881
1431	56.6	.463	.532	.592	.633	.626	.613	.591	.636	.578	.601
1526	47.4	.505	.575	.662	.700	.714	.727	.731	.811	.832	.872
1601	41.1	.274	.309	.347	.373	.377	.373	.393	.432	.470	.474

Table 6.- Concluded.

Time EDT	Solar Alt (deg)	Aerosol optical depths at specified wavelengths (nm). 400	440	490	520	550	580	610	670	700	750
1319	65.5	.244	.236	.195	.167	.175	.169	.196	.124	.092	.079
1330	64.5	.245	.242	.198	.174	.175	.177	.191	.127	.097	.078
1403	60.7	.264	.255	.206	.173	.176	.184	.198	.127	.100	.088
1431	56.6	.407	.384	.358	.317	.345	.375	.426	.391	.483	.470
1526	47.4	.322	.305	.247	.217	.212	.205	.213	.148	.118	.098
1601	41.1	.934	.928	.891	.845	.852	.872	.834	.778	.689	.708

WAVE LENGTH (NM)	AVG OPT DEPTH	RAY OPT DEP	OZONE OPT DEP	AERO OPT DEP	STD DEV OPD	AVG TOT TRANS	STD DEV TRANS
400	.613	.349	.013	.251	.009	.542	.005
440	.491	.235	.012	.244	.008	.612	.005
490	.366	.151	.015	.200	.004	.694	.003
520	.312	.118	.022	.171	.003	.732	.002
550	.299	.094	.030	.175	.000	.741	.000
580	.290	.076	.038	.177	.006	.748	.005
610	.295	.062	.038	.195	.003	.745	.002
670	.187	.042	.019	.126	.001	.829	.001
700	.162	.035	.030	.097	.003	.851	.003
750	.121	.027	.012	.082	.005	.886	.004

Table 7.- Atmospheric optical properties for May 14, 1981.

Time EDT	Solar Alt (deg)	Total optical depths at specified wavelengths (nm). 400	440	490	520	550	580	610	670	700	750
545	3.0	.602	.608	.638	.661	.684	.696	.724	.777	.781	.819
600	5.6	.524	.554	.610	.639	.663	.676	.704	.762	.766	.808
615	8.3	.430	.483	.557	.591	.618	.633	.663	.729	.733	.782
630	11.0	.413	.482	.563	.601	.622	.636	.645	.732	.738	.789
645	13.7	.411	.483	.566	.599	.624	.637	.663	.732	.736	.786
659	16.3	.379	.450	.532	.568	.594	.609	.634	.708	.712	.766
715	19.3	.384	.456	.539	.573	.599	.613	.638	.711	.714	.763
730	22.1	.378	.443	.526	.560	.584	.598	.620	.692	.701	.752
747	25.3	.384	.454	.539	.574	.603	.615	.638	.714	.716	.774
800	27.7	.388	.461	.544	.578	.605	.618	.639	.716	.720	.777
834	34.1	.412	.481	.568	.601	.622	.635	.653	.732	.743	.797
901	39.1	.420	.491	.575	.610	.630	.643	.656	.738	.744	.792
933	45.0	.427	.497	.581	.615	.633	.650	.662	.746	.744	.793
1001	50.0	.430	.499	.585	.618	.636	.654	.662	.744	.752	.798
1030	54.9	.413	.481	.564	.599	.624	.637	.645	.731	.738	.788
1105	60.2	.394	.462	.538	.516	.593	.601	.637	.413	.828	.832
1130	63.3	.410	.479	.566	.602	.632	.646	.650	.739	.748	.796
1200	66.1	.417	.494	.581	.619	.638	.652	.655	.743	.756	.807

Table 7.- Continued

Time EDT	Solar Alt (deg)	Total transmittances at specified wavelengths (nm). 400	440	490	520	550	580	610	670	700	750
545	3.0	.507	.498	.449	.414	.380	.362	.323	.252	.247	.200
600	5.6	.645	.591	.494	.448	.411	.392	.351	.272	.267	.213
615	8.3	.844	.727	.584	.526	.481	.457	.411	.317	.310	.246
630	11.0	.885	.731	.574	.509	.474	.452	.438	.313	.304	.238
645	13.7	.889	.728	.569	.513	.472	.451	.410	.312	.307	.240
659	16.3	.969	.799	.631	.565	.521	.497	.455	.345	.339	.266
715	19.3	.957	.786	.618	.557	.513	.489	.449	.342	.337	.265
730	22.1	.973	.814	.643	.580	.539	.515	.479	.368	.356	.286
747	25.3	.957	.789	.618	.556	.505	.487	.450	.337	.334	.256
800	27.7	.947	.774	.609	.549	.502	.482	.448	.334	.329	.252
834	34.1	.887	.732	.566	.510	.475	.454	.427	.312	.297	.231
901	39.1	.868	.711	.553	.494	.462	.442	.422	.303	.296	.233
933	45.0	.851	.699	.542	.487	.457	.431	.412	.293	.296	.233
1001	50.0	.844	.694	.536	.481	.452	.425	.413	.296	.285	.225
1030	54.9	.885	.733	.573	.513	.472	.451	.438	.313	.304	.239
1105	60.2	.932	.773	.620	.663	.523	.509	.452	.884	.189	.184
1130	63.3	.891	.736	.569	.508	.459	.436	.430	.303	.290	.228
1200	66.1	.875	.705	.543	.480	.450	.428	.424	.296	.279	.214

Table 7.- Concluded.

Time EDT	Solar Alt (deg)	Aerosol optical depths at specified wavelengths (nm). 400	440	490	520	550	580	610	670	700	750
545	3.0	.145	.251	.283	.273	.256	.249	.223	.191	.181	.161
600	5.6	.283	.344	.328	.307	.286	.278	.252	.210	.201	.174
615	8.3	.481	.480	.418	.386	.356	.343	.312	.255	.245	.207
630	11.0	.523	.483	.408	.369	.350	.338	.339	.251	.239	.199
645	13.7	.527	.480	.403	.372	.348	.337	.311	.251	.242	.201
659	16.3	.607	.552	.465	.425	.397	.383	.355	.284	.274	.228
715	19.3	.595	.539	.452	.416	.389	.375	.349	.280	.272	.226
730	22.1	.611	.567	.477	.439	.414	.401	.379	.306	.290	.247
747	25.3	.595	.541	.452	.415	.381	.373	.350	.276	.269	.217
800	27.7	.584	.527	.443	.408	.378	.368	.348	.273	.264	.213
834	34.1	.525	.485	.400	.369	.350	.340	.327	.251	.232	.193
901	39.1	.506	.463	.387	.353	.338	.328	.322	.242	.230	.194
933	45.0	.489	.452	.376	.346	.333	.317	.312	.232	.231	.194
1001	50.0	.482	.447	.370	.340	.328	.311	.313	.234	.220	.186
1030	54.9	.522	.485	.407	.373	.347	.337	.338	.252	.238	.200
1105	60.2	.570	.525	.454	.522	.398	.395	.352	.823	.124	.145
1130	63.3	.529	.489	.403	.368	.334	.323	.330	.242	.225	.189
1200	66.1	.512	.458	.377	.340	.325	.314	.324	.235	.214	.175

WAVE LENGTH (NM)	AVG OPT DEPTH	RAY OPT DEP	OZONE OPT DEP	AERO OPT DEP	STD DEV OPD	AVG TOT TRANS	STD DEV TRANS
400	.909	.349	.013	.547	.046	.403	.018
440	.749	.235	.012	.502	.039	.473	.019
490	.586	.151	.015	.420	.035	.557	.019
520	.526	.118	.022	.385	.032	.591	.019
550	.487	.094	.030	.363	.027	.615	.016
580	.464	.076	.038	.351	.027	.629	.017
610	.437	.062	.038	.337	.020	.646	.013
670	.322	.042	.019	.261	.022	.725	.016
700	.315	.035	.030	.250	.022	.730	.016
750	.247	.027	.012	.208	.017	.781	.013

Table 8.- Normalized sky radiance distributions for May 7, 1981.

Time EDT	Solar Alt (deg)	Airmass	Scattering Angle (deg)	Normalized* sky radiance at specified wavelengths (nm). 400	440	490	520	550	580	610	670	700	750
1240	65.7	8.453	84.1	.469	.370	.281	.256	.205	.202	.192	.152	.152	.147
1244	65.6	2.016	63.3	.735	.694	.684	.674	.678	.687	.687	.689	.710	.709
1248	65.5	1.313	46.2	1.008	1.000	.974	.973	.988	.977	.981	.991	1.000	.977
1251	65.5	1.087	33.2	1.265	1.272	1.259	1.256	1.267	1.264	1.244	1.254	1.273	1.211
1254	65.4	1.000	24.6	1.507	1.534	1.555	1.551	1.568	1.553	1.537	1.560	1.527	1.472
1258	65.2	1.111	35.3	1 477	1.560	1.648	1.661	1.711	1.696	1.680	1.743	1.731	1.680
1302	65.1	1.313	46.4	1.276	1.399	1.519	1.570	1.644	1.644	1.653	1.749	1.718	1.713
1305	64.9	1.946	62.4	651	.727	.848	.911	.892	1.017	1.095	1.223	1.208	1.416

May 7 Normal-plane scan.

Time EDT	Solar Alt (deg)	Airmass	Scattering Angle (deg)	Normalized* sky radiance at specified wavelengths (nm). 400	440	490	520	550	580	610	670	700	750
1335	62.6	8.773	56.5	.862	.859	.872	.890	.816	.834	.858	.780	.744	.784
1338	62.3	2.067	33.5	1.311	1.338	1.372	1.377	1.400	1.405	1.401	1.427	1.439	1.443
1341	62.0	1.327	13.2	2.163	2.368	2.620	2.721	2.947	3.063	3.179	3.476	3.550	3.701
1344	61.7	1.062	8.6	4.187	4.916	5.553	5.732	6.213	6.307	6.565	7.314	7.449	7.902
1348	61.3	1.000	29.6	1.432	1.521	1.617	1.633	1.730	1.741	1.775	1.936	1.939	1.980
1351	60.9	1.057	48.1	.991	1.053	1.134	1.164	1.247	1.290	1.308	1.483	1.510	1.558
1354	60.6	1.302	69.3	.792	.882	1.025	1.111	1.246	1.325	1.395	1.573	1.630	1.799
1357	60.2	1.940	88.9	.561	.508	.460	.433	.418	.399	.375	.353	.350	.340
1400	59.8	3.562	104.1	.564	.502	.434	.411	.376	.355	.344	.303	.290	.286

May 7 Sun-plane scan.

*Normalized by sky radiance at $\phi = 45^{\circ}$.

Table 9.- Normalized sky radiance distributions for May 8, 1981.

Time EDT	Solar Alt (deg)	Airmass	Scattering Angle (deg)	Normalized* sky radiance at specified wavelengths (nm). 400	440	490	520	550	580	610	670	700	750
945	46.1	8.186	39.5	1.175	1.250	1.270	1.278	1.181	1.197	1.212	1.119	1.054	1.032
950	47.0	1.940	16.1	2.066	2.224	2.394	2.436	2.564	2.662	2.718	2.937	2.909	2.844
955	47.8	1.300	2.4	10.124	12.788	16.391	18.599	20.527	23.515	24.067	26.938	28.098	27.804
1000	48.7	1.070	20.4	1.729	1.835	1.952	1.984	2.110	2.137	2.186	2.312	2.346	2.278
1015	51.2	1.000	37.8	1.159	1.206	1.247	1.237	1.289	1.300	1.290	1.355	1.367	1.327
1022	52.4	1.062	57.3	.753	.741	.746	.754	.800	.815	.816	.845	.879	.916
1025	52.9	1.951	96.4	.601	.540	.486	.471	.449	.431	.420	.397	.398	.396

May 8 Sun-plane scan.

Time EDT	Solar Alt (deg)	Airmass	Scattering Angle (deg)	Normalized* sky radiance at specified wavelengths (nm). 400	440	490	520	550	580	610	670	700	750
1315	64.6	1.000	26.5	1.465	1.487	1.531	1.524	1.596	1.596	1.589	1.653	1.641	1.635
1319	64.3	1.062	45.4	.966	.982	1.001	1.013	1.053	1.057	1.051	1.087	1.110	1.096
1324	63.9	1.300	65.9	.810	.869	.968	1.006	1.080	1 126	1.157	1.259	1.306	1.397
1328	63.5	2.023	87.0	.577	.511	.454	.428	.406	.392	.371	.344	.339	.323
1333	63.1	5.600	106.9	.589	.540	.480	.463	.416	.407	.405	.366	.359	.355
1337	62.7	1.062	7.5	4.780	5.496	6.360	6.623	7.109	7.392	7.575	8.332	8.528	8.440
1342	62.2	1.313	12.7	2.356	2.534	2.775	2.878	3.089	3.216	3.314	3.642	3.773	3.779
1346	61.7	1.992	31.7	1.362	1.363	1.354	1.357	1.351	1.344	1.325	1.331	1.317	1.274
1350	61.3	5.548	51.2	.857	.885	.896	.898	.846	.854	.871	.816	.806	.806

May 8 Sun-plane scan.

*Normalized by sky radiance at $\phi = 45^o$.

Table 10.- Normalized sky radiance distributions for May 8 and 13, 1981.

Time EDT	Solar Alt (deg)	Airmass	Scattering Angle (deg)	Normalized* sky radiance at specified wavelengths (nm).									
				400	440	490	520	550	580	610	670	700	750
1556	41.2	6.306	130.0	.598	.539	.472	.455	.403	.388	.394	.303	.301	.289
1600	40.5	2.016	109.9	.566	.488	.414	.380	.358	.332	.312	.282	.266	.252
1604	39.7	1.313	90.8	.533	.474	.417	.394	.377	.358	.337	.324	.317	.290
1608	39.0	1.061	70.6	.684	.712	.768	.804	.854	.892	.889	1.008	1.025	1.088
1612	38.2	1.000	51.9	.842	.862	.907	.921	.953	.981	.958	1.029	1.040	1.056
1617	37.3	1.190	19.8	1.795	1.913	2.025	2.069	2.182	2.226	2.246	2.493	2.512	2.531
1621	36.6	1.311	13.0	2.492	2.774	3.141	3.286	3.550	3.722	3.832	4.343	4.451	4.508
1624	36.0	2.035	6.7	4.946	5.688	6.155	6.221	6.323	6.428	6.442	6.986	7.343	7.697
1627	35.5	5.548	25.4	1.412	1.521	1.589	1.642	1.598	1.628	1.749	1.559	1.613	1.650

May 8 Sun-plane scan.

Time EDT	Solar Alt (deg)	Airmass	Scattering Angle (deg)	Normalized* sky radiance at specified wavelengths (nm).									
				400	440	490	520	550	580	610	670	700	750
1229	67.2	5.548	80.7	.612	.583	.535	.504	.505	.491	.506	.444	.420	.418
1234	67.2	2.016	62.9	.759	.721	.684	.669	.653	.638	.641	.632	.635	.629
1238	67.2	1.313	45.5	.989	.978	.974	.984	.971	.972	.957	.982	.993	.999
1243	67.2	1.062	29.8	1.440	1.494	1.564	1.596	1.622	1.660	1.635	1.737	1.752	1.766
1247	67.1	1.000	22.9	1.697	1.786	1.899	1.935	1.918	1.992	1.990	2.115	2.147	2.139
1250	67.0	1.061	29.9	1.410	1.480	1.538	1.594	1.598	1.625	1.644	1.682	1.725	1.742
1255	66.9	1.289	44.5	1.027	1.034	1.045	1.061	1.049	1.072	1.043	1.077	1.077	1.058
1301	66.6	1.992	62.6	.781	.746	.724	.723	.712	.701	.688	.679	.670	.670
1305	66.4	5.497	80.7	.590	.587	.571	.568	.582	.566	.595	.534	.505	.540

May 13 Normal-plane scan.

*Normalized by sky radiance at $\phi = 45^{\circ}$.

Table 11.- Normalized sky radiance distributions for May 14, 1981.

Time EDT	Solar Alt (deg)	Airmass	Scattering Angle (deg)	Normalized* sky radiance at specified wavelengths (nm). 400	440	490	520	550	580	610	670	700	750
812	30.0	5.600	85.0	.567	.604	.593	.610	.598	.592	.597	.473	.424	.423
814	30.3	2.023	75.6	.681	.698	.667	.666	.648	.635	.626	.537	.504	.494
816	30.7	1.313	67.1	732	.757	.725	.733	.710	.710	.711	.634	.602	.592
818	31.1	1.062	60.9	.761	.784	.780	.792	.784	.786	.781	.706	.672	.679
820	31.5	1.000	58.5	.785	.812	.821	.831	.831	.826	.831	.758	.723	.716
822	31.8	1.063	60.3	.788	.813	.805	.813	.822	.813	.817	.734	.698	.694
826	32.6	1.289	65.3	.763	.775	.761	.764	.751	.737	.744	.652	.603	.600
828	33.0	1.992	74.2	.728	.737	.702	.697	.687	.670	.655	.556	.506	.499
830	33.3	5.548	84.5	.591	.635	.634	.657	.656	.647	.663	.533	.466	.467

May 14 Normal-plane scan.

Time EDT	Solar Alt (deg)	Airmass	Scattering Angle (deg)	Normalized* sky radiance at specified wavelengths (nm). 400	440	490	520	550	580	610	670	700	750
910	40.8	1.000	48.2	975	.961	.942	.941	.934	.921	.922	.911	.913	.920
913	41.3	1.015	58.6	.822	.785	.748	.734	.714	.716	.703	.694	.700	.709
916	41.9	1.062	67.8	.736	.683	.627	.611	.587	.582	.576	.576	.569	.588
917	42.1	1.156	78.1	.673	.611	.543	.521	.499	.484	.477	.468	.468	.485
920	42.6	1.313	87.9	.651	.575	.499	.480	.452	.436	.426	.408	.412	.429
923	43.2	1.540	96.4	.651	.577	.493	.470	.440	.419	.404	.376	.376	.388
925	43.5	1.992	106.5	.653	.588	.504	.475	.444	.420	.405	.371	.359	.390
928	44.1	2.956	116.3	.651	.590	.518	.493	.470	.442	.424	.378	.365	.393
930	44.4	5.600	125.6	.568	.548	.494	.481	.474	457	.460	.392	.373	.418

May 14 Sun-plane scan.

*Normalized by sky radiance at $\phi = 45^o$.

Table 12.- Normalized sky radiance distributions for May 14, 1981.

Time EDT	Solar Alt (deg)	Airmass	Scattering Angle (deg)	Normalized* sky radiance at specified wavelengths (nm). 400	440	490	520	550	580	610	670	700	750
1213	66.9	1.000	22.2	1.868	1.988	2.132	2.124	2.133	2.140	2.106	2.112	2.102	2.098
1215	67.0	1.015	33.0	1.350	1.416	1.490	1.487	1.500	1.494	1.495	1.489	1.469	1.475
1218	67.1	1.062	42.6	1.037	1.053	1.074	1.075	1.081	1.082	1.075	1.079	1.079	1.062
1219	67.2	1.156	53.0	.830	.814	.761	.790	.793	.795	.790	.782	.781	.781
1221	67.2	1.313	63.3	.718	.688	.669	.659	.655	.654	.663	.670	.668	.660
1224	67.3	1.536	72.2	.693	.661	.641	.624	.618	.621	.629	.628	.623	.645
1226	67.4	1.992	82.6	.754	.776	.834	.853	.909	.928	.957	.994	.988	1.112

May 14 Sun-plane scan.

*Normalized by sky radiance at $\phi = 45^{o}$.

Total and sky

Table 13.- Irradiance properties on May 7, 1981.

Time EDT	Solar Alt (deg)	Irradiance Type	Irradiance ($\mu\omega cm^{-2} nm^{-1}$) or irradiance ratio at specified wavelengths (nm).									
			400	440	490	520	550	580	610	670	700	750
1150	63.7	H	99.1	136.8	157.5	150.1	153.2	149.1	142.1	134.9	126.7	115.6
		HSKY	*	*	*	*	*	*	*	*	*	*
		HSKY/H	*	*	*	*	*	*	*	*	*	*
1317	64.2	H	94.9	131.6	150.5	141.7	146.2	142.1	135.7	128.9	121.6	110.2
		HSKY	27.8	35.1	26.4	22.1	19.4	16.8	14.4	11.6	10.3	8.6
		HSKY/H	.293	.266	.175	.156	.133	.118	.106	.090	.084	.078
1405	59.2	H	89.8	124.2	144.3	137.3	139.4	135.6	129.2	123.0	116.1	104.5
		HSKY	26.9	29.8	25.9	21.6	18.9	16.4	14.0	11.2	9.9	8.1
		HSKY/H	.299	.240	.179	.157	.135	.121	.108	.091	.085	.078
1500	50.8	H	76.2	108.0	125.2	119.1	120.4	116.7	111.3	105.8	99.7	89.3
		HSKY	24.7	27.7	24.2	19.9	17.6	15.1	13.0	10.5	9.2	7.5
		HSKY/H	.324	.257	.193	.167	.146	.130	.117	.099	.092	.083
1554	41.4	H	62.3	87.9	101.4	96.6	97.5	94.2	90.0	86.1	81.0	72.4
		HSKY	23.4	26.0	22.9	19.0	16.7	14.5	12.4	10.1	8.9	7.3
		HSKY/H	.375	.296	.226	.197	.171	.153	.138	.117	.109	.101

Table 14.- Total and sky irradiance properties on May 8, 1981.

Time EDT	Solar Alt (deg)	Irradiance Type	Irradiance ($\mu w cm^{-2} nm^{-1}$) or irradiance ratio at specified wavelengths (nm). 400	440	490	520	550	580	610	670	700	750
910	39.8	H	55.2	78.1	90.7	86.8	87.7	84.9	81.3	78.5	73.4	67.0
		HSKY	26.6	31.6	29.3	25.3	23.3	22.2	18.0	15.0	13.6	11.5
		HSKY/H	.483	.404	.323	.291	.265	.262	.221	.192	.185	.171
1107	59.2	H	87.1	122.2	140.0	133.9	135.4	131.8	125.6	119.6	112.0	101.7
		HSKY	31.3	36.1	34.0	28.2	25.5	22.7	20.0	16.9	15.1	12.9
		HSKY/H	.360	.295	.243	.211	.189	.172	.160	.141	.135	.127
1213	65.4	H	92.0	127.7	146.3	139.6	141.5	138.6	131.6	126.0	117.9	107.8
		HSKY	*	*	*	*	*	*	*	*	*	*
		HSKY/H	*	*	*	*	*	*	*	*	*	*
1310	64.9	H	91.3	127.5	145.5	138.8	140.7	136.9	130.1	124.2	116.2	106.0
		HSKY	32.6	37.4	34.0	29.0	26.2	23.2	20.3	17.1	15.1	12.7
		HSKY/H	.357	.293	.233	.209	.186	.170	.156	.138	.130	.120
1402	59.8	H	86.7	121.0	139.0	132.5	134.1	131.2	124.5	118.9	111.1	101.5
		HSKY	*	*	*	*	*	*	*	*	*	*
		HSKY/H	*	*	*	*	*	*	*	*	*	*
1547	42.8	H	61.8	88.4	102.0	97.1	98.2	94.7	90.7	87.3	81.5	74.5
		HSKY	29.7	35.4	33.4	28.8	26.4	23.6	21.2	18.2	16.4	14.3
		HSKY/H	.480	.400	.327	.297	.269	.249	.234	.208	.201	.192

Table 15.- Total and sky irradiance properties on May 9, 13, 14, 1981.

Time EDT	Solar Alt (deg)	Irradiance Type	Irradiance ($\mu w cm^{-2} nm^{-1}$) or irradiance ratio at specified wavelengths (nm). 400	440	490	520	550	580	610	670	700	750
						May 9						
906	39.2	H	55.9	78.6	92.4	86.8	88.2	85.1	81.6	78.3	73.0	66.5
		HSKY	*	*	*	*	*	*	*	*	*	*
		HSKY/H	*	*	*	*	*	*	*	*	*	*
1006	49.9	H	72.7	99.6	116.1	110.8	112.3	109.1	104.1	99.0	92.7	84.6
		HSKY	26.9	31.9	28.1	23.9	21.6	18.9	16.4	13.7	12.1	11.2
		HSKY/H	.370	.320	.243	.216	.193	.173	.157	.138	.130	.132
1105	59.1	H	85.2	118.2	135.7	129.6	131.6	127.9	121.9	115.7	108.4	99.3
		HSKY	*	*	*	*	*	*	*	*	*	*
		HSKY/H	*	*	*	*	*	*	*	*	*	*
						May 13						
1530	46.7	H	63.1	88.4	99.0	94.2	91.6	85.5	85.5	82.6	74.0	70.6
		HSKY	*	*	*	*	*	*	*	*	*	*
		HSKY/H	*	*	*	*	*	*	*	*	*	*
						May 14						
905	39.9	H	52.8	75.9	88.2	84.7	85.8	83.4	80.6	78.1	70.0	66.4
		HSKY	31.4	38.9	37.2	32.1	29.2	25.9	22.8	19.0	15.9	13.9
		HSKY/H	.594	.513	.421	.379	.340	.310	.283	.243	.227	.209
1005	50.7	H	67.7	96.4	112.0	107.2	109.1	106.1	101.8	97.7	88.6	83.5
		HSKY	34.5	42.0	40.1	34.7	31.5	28.0	24.5	20.3	17.2	14.9
		HSKY/H	.510	.435	.358	.324	.289	.264	.241	.208	.194	.178
1204	66.4	H	87.1	122.4	141.2	135.6	137.7	134.6	128.8	123.5	112.3	106.1
		HSKY	40.8	47.4	44.6	38.2	34.6	30.4	26.9	21.8	18.3	15.7
		HSKY/H	.468	.387	.316	.282	.251	.226	.209	.177	.163	.148

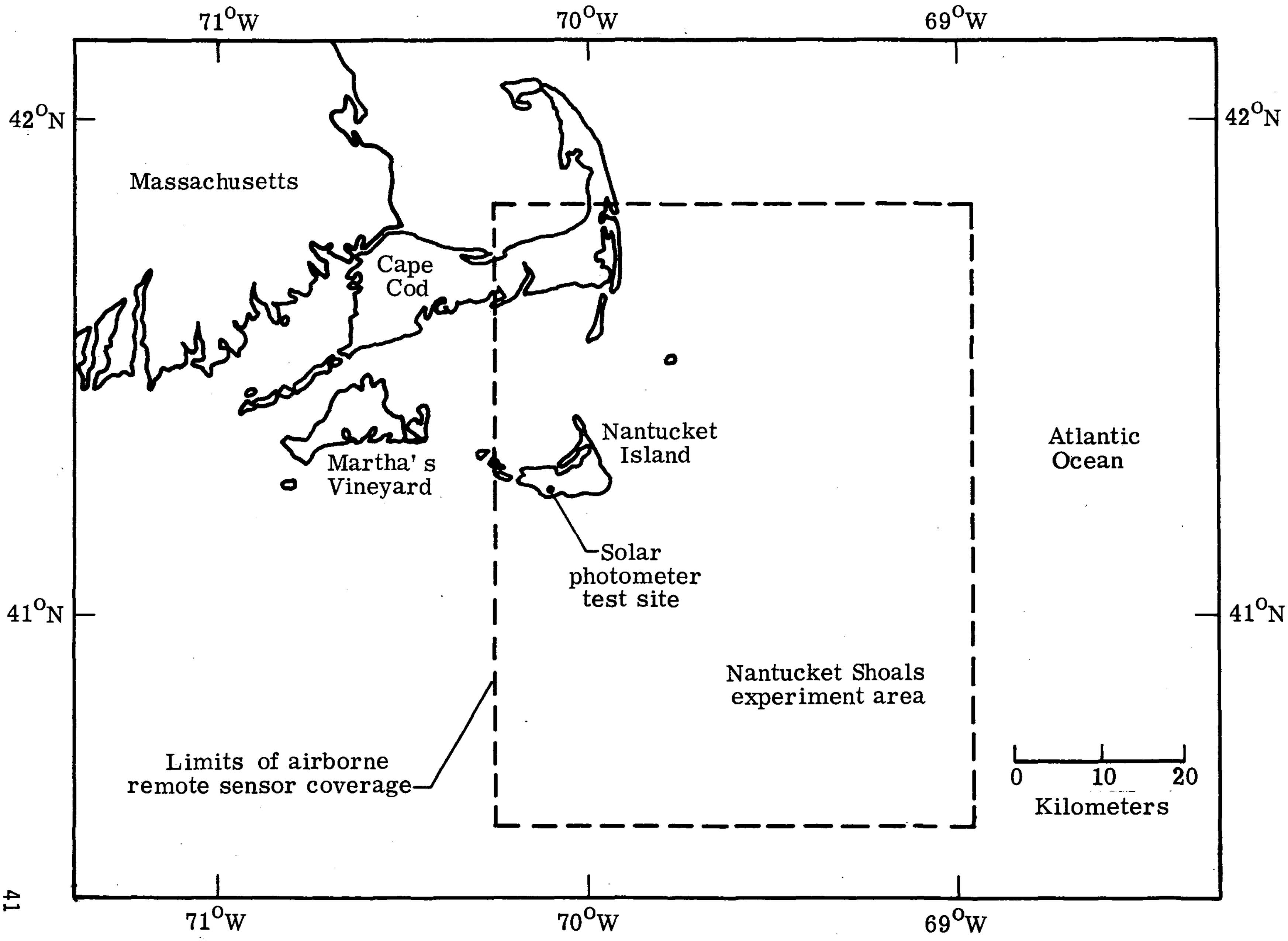

Figure 1.- Nantucket Shoals area test site.

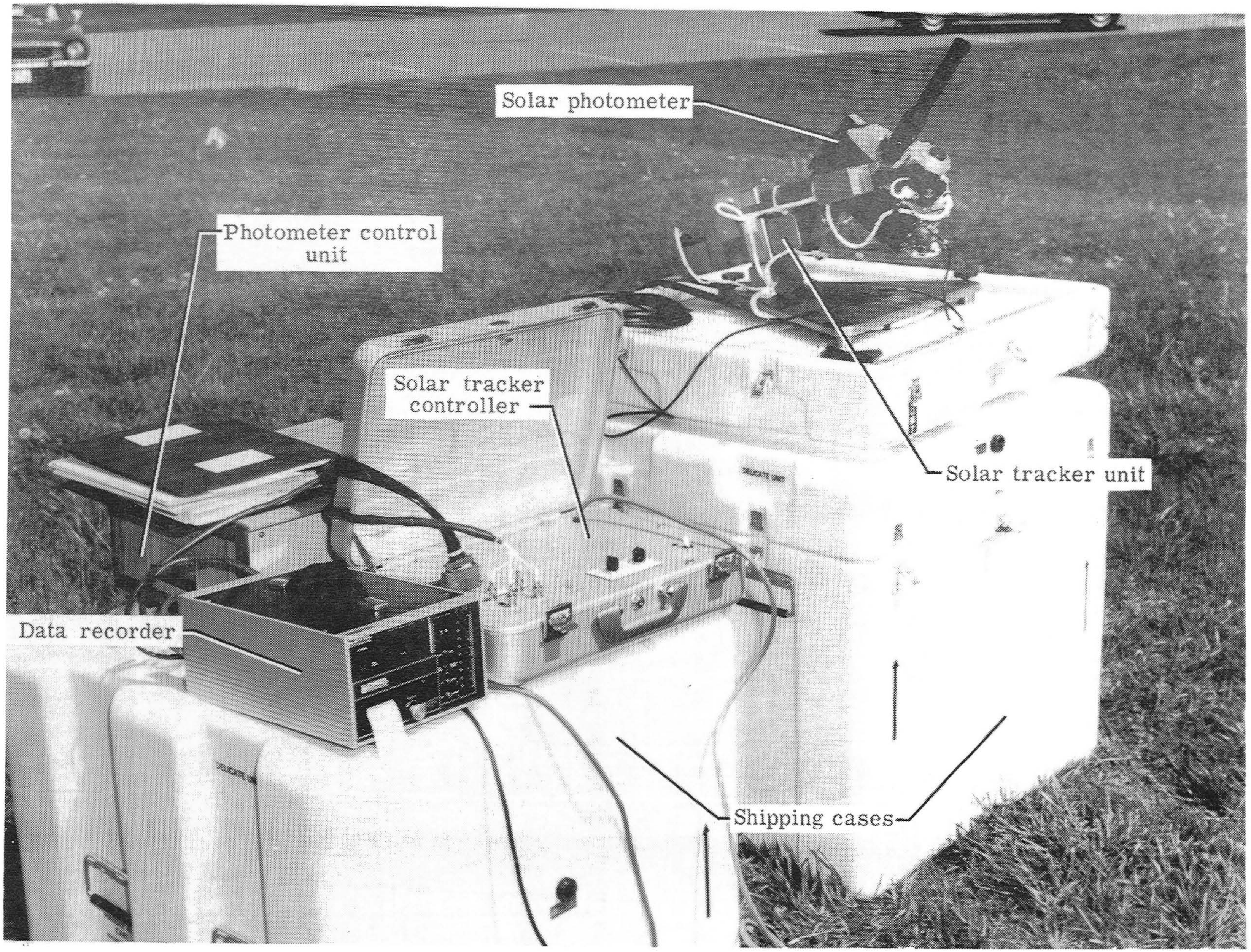

Figure 2.- Solar photometer system.

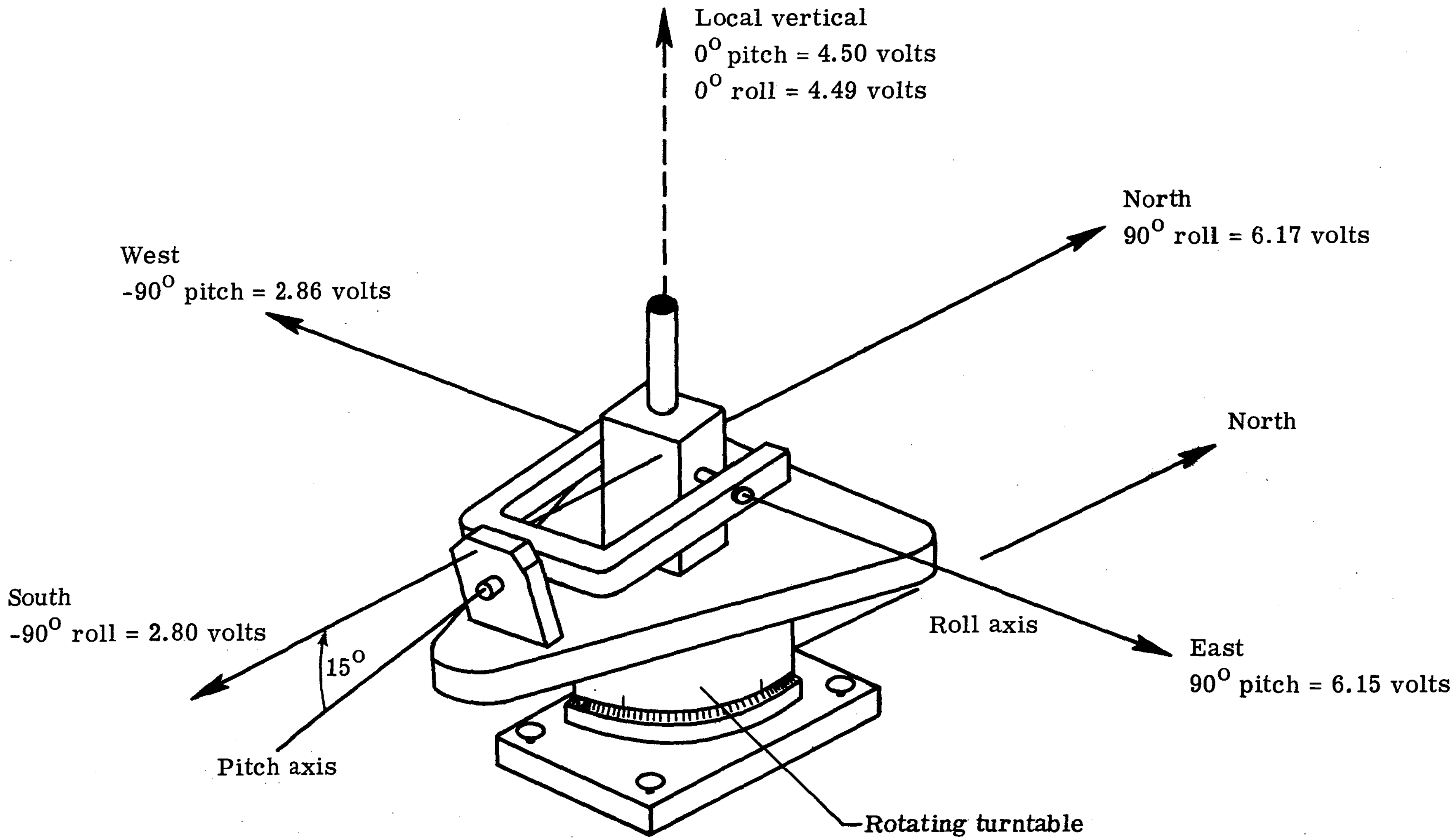

Figure 3.- Solar tracker alignment.

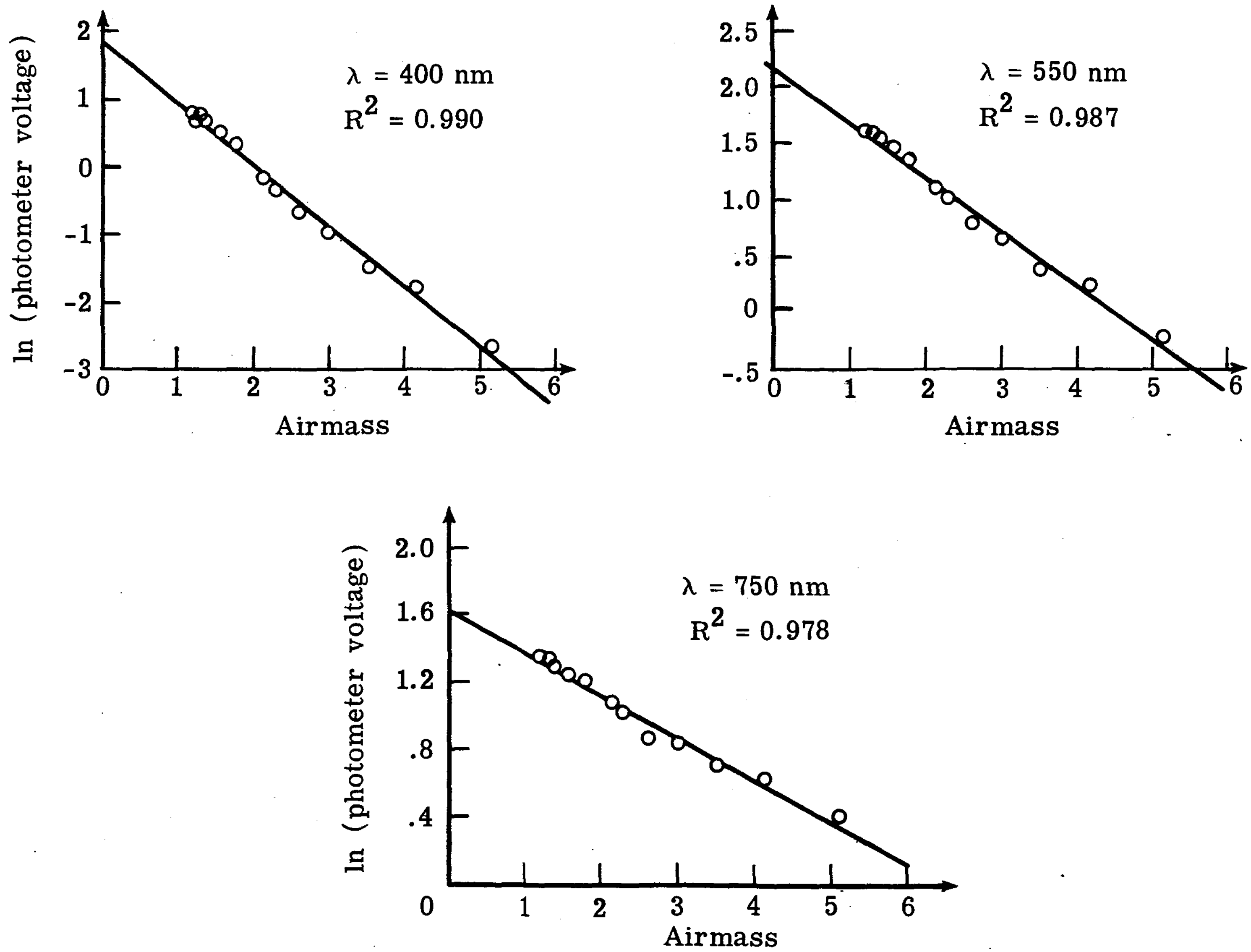

Figure 4.- Langley plot method for May 14, 1981 photometer data.

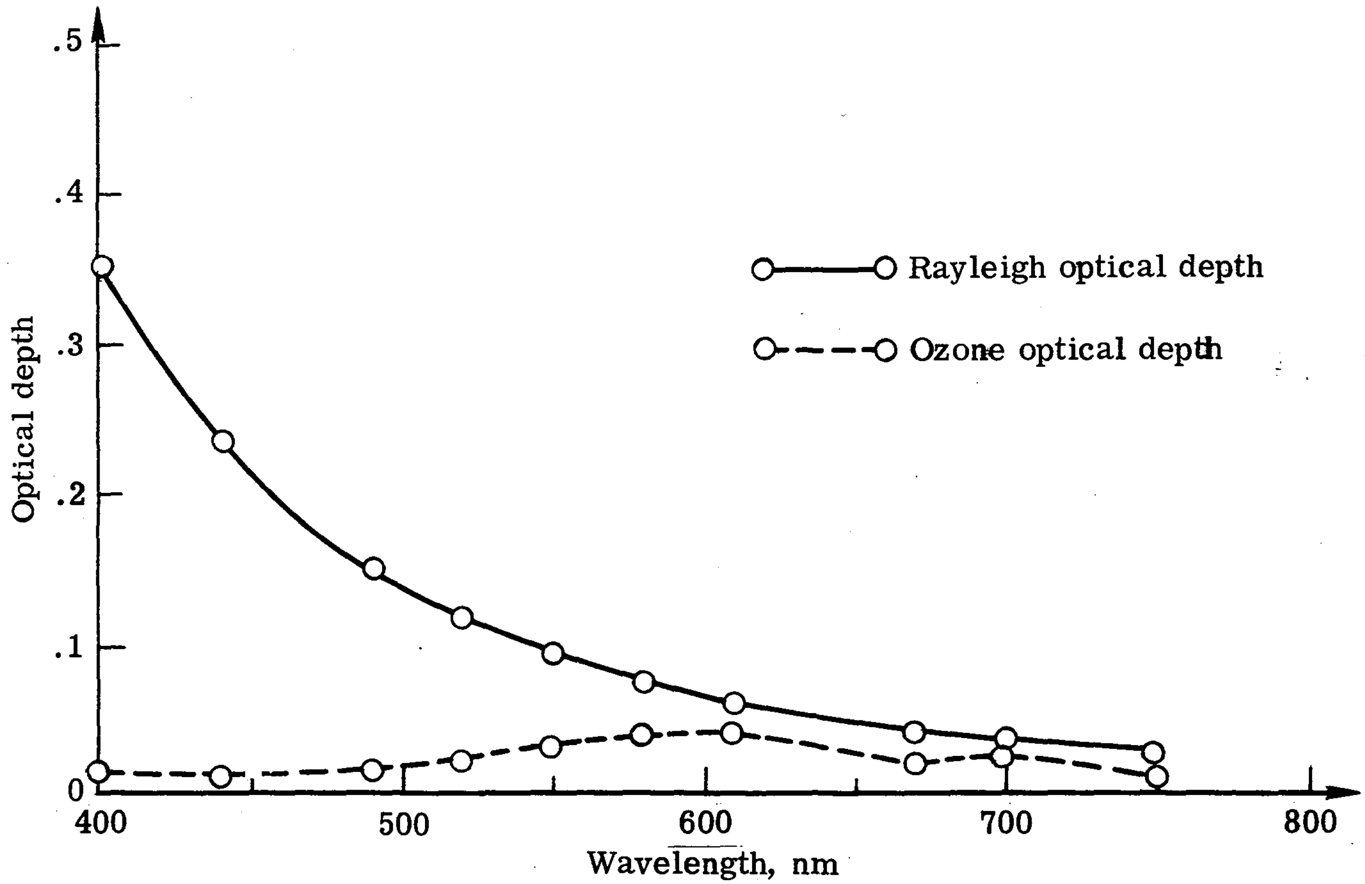

Figure 5.- Rayleigh and ozone optical depths.

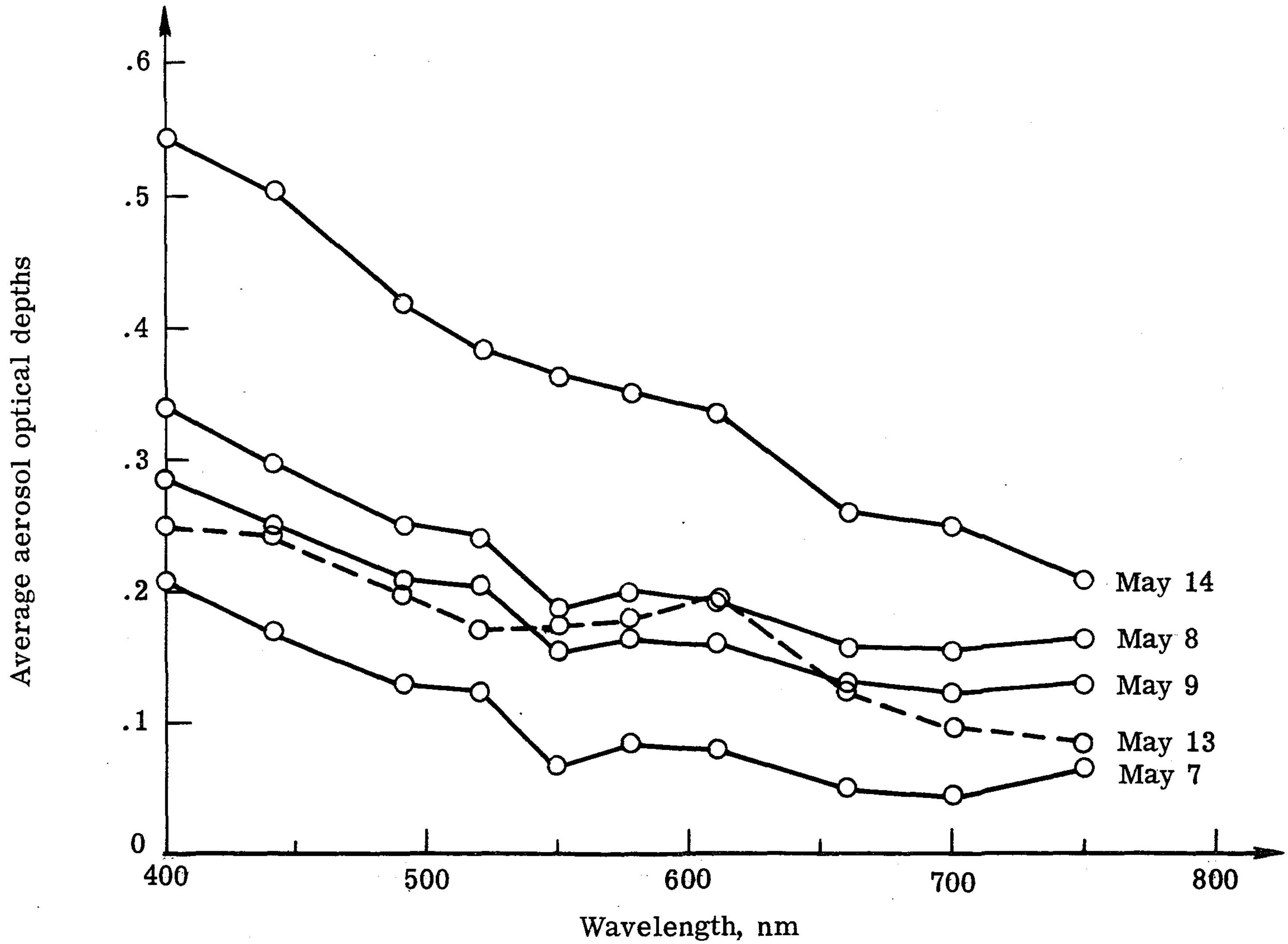

Figure 6.- Average aerosol optical depths for May 7-14, 1981.

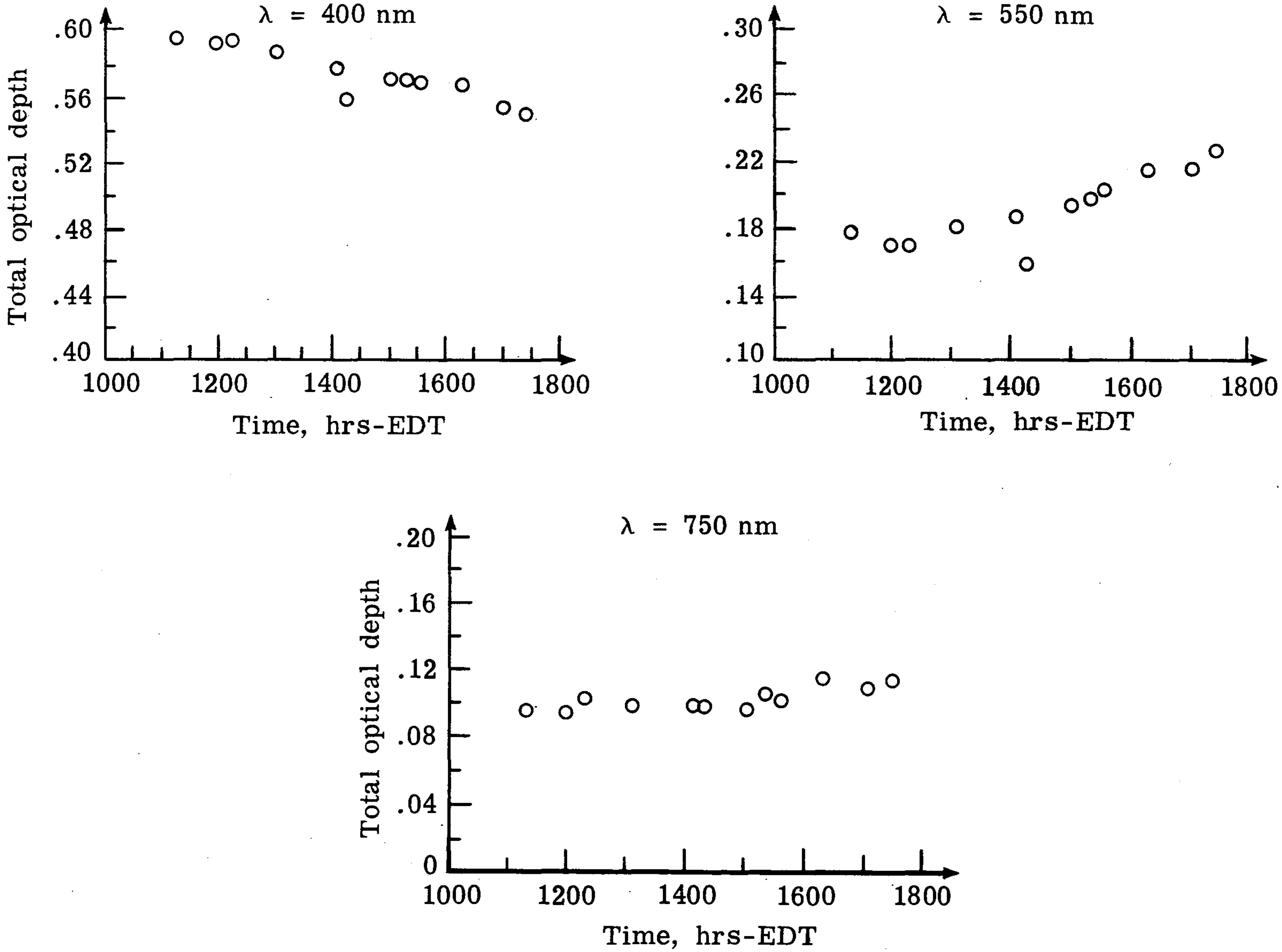

Figure 7(a).- Total optical depth histories for May 7, 1981.

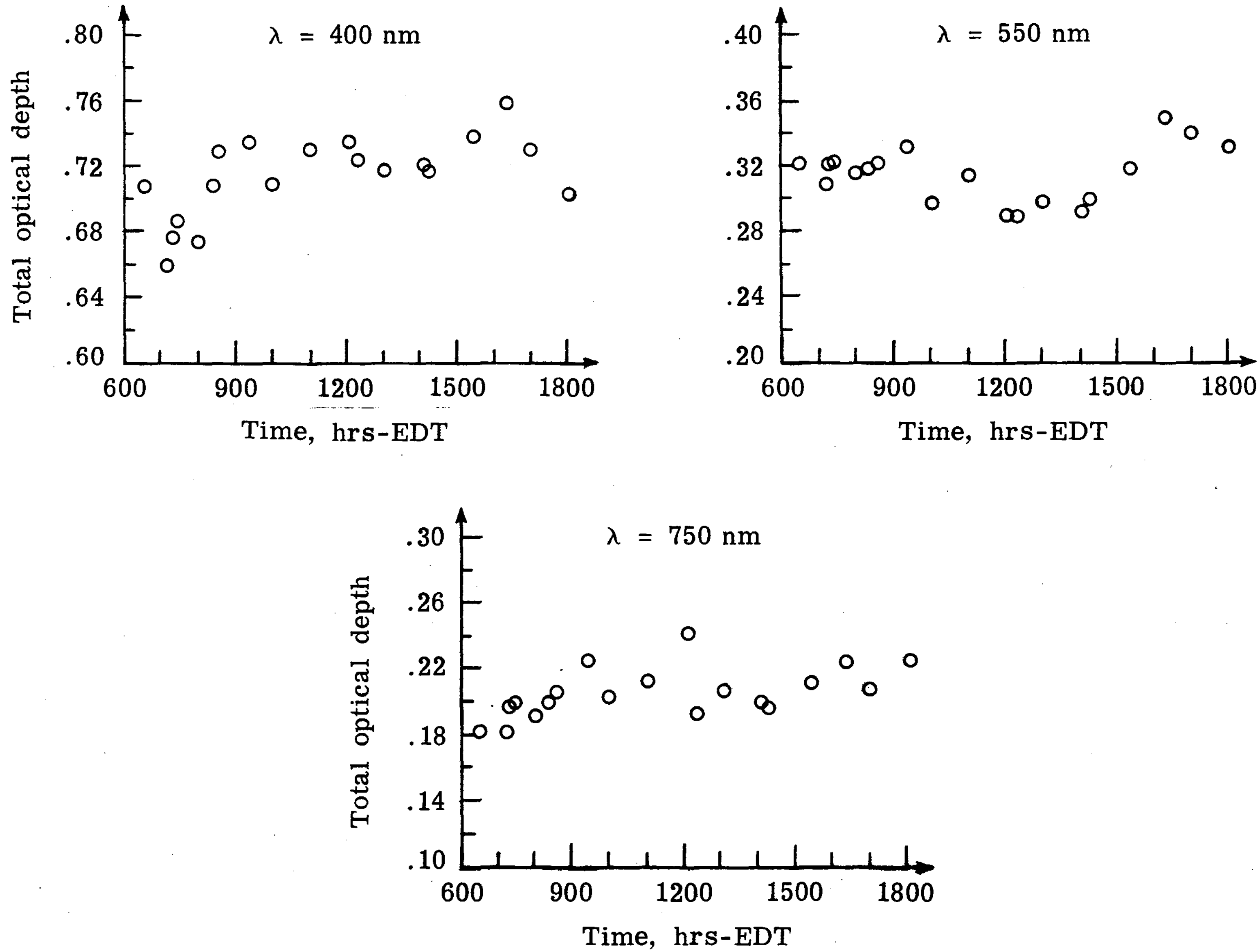

Figure 7(b).- Total optical depth histories for May 8, 1981.

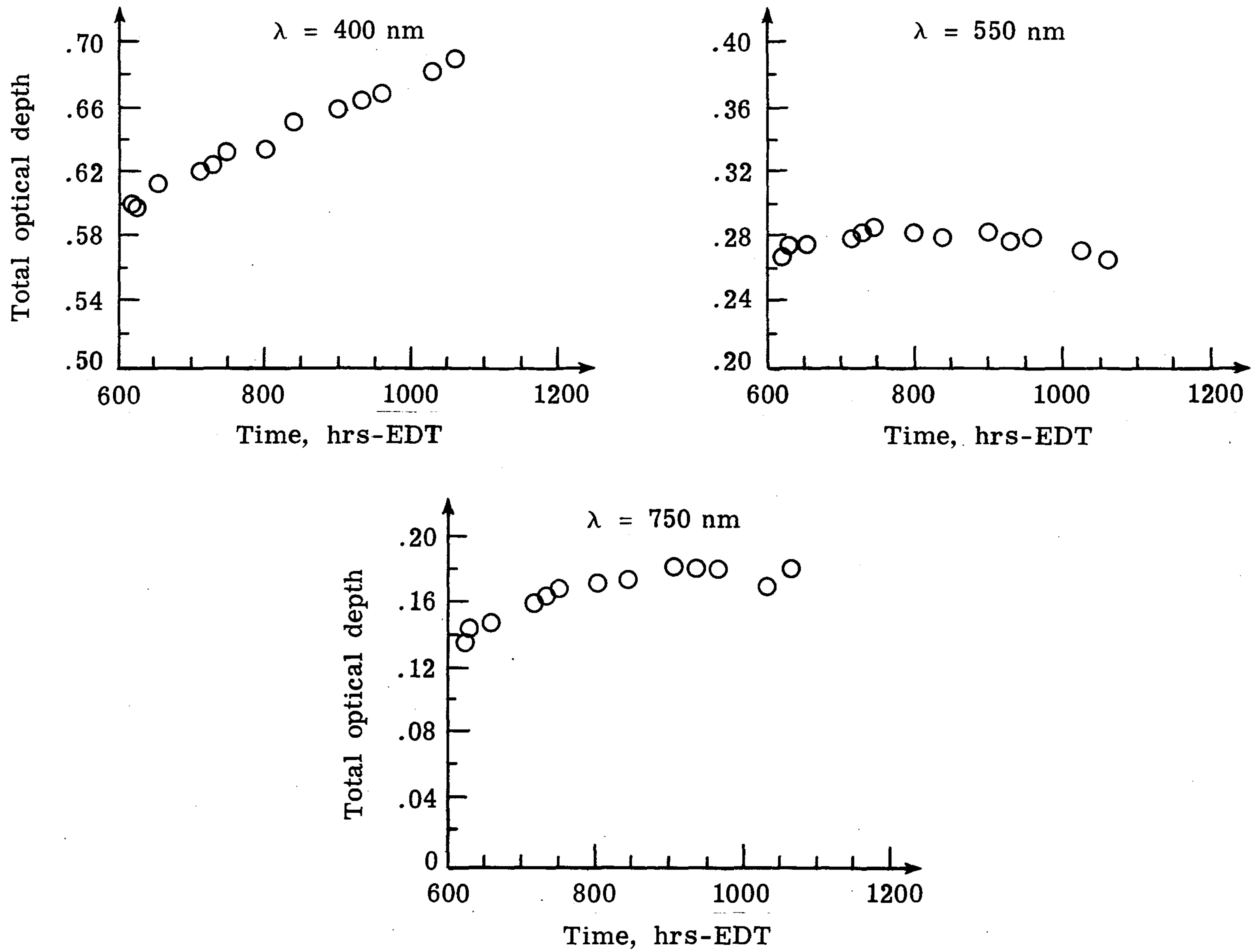

Figure 7(c).- Total optical depth histories for May 9, 1981.

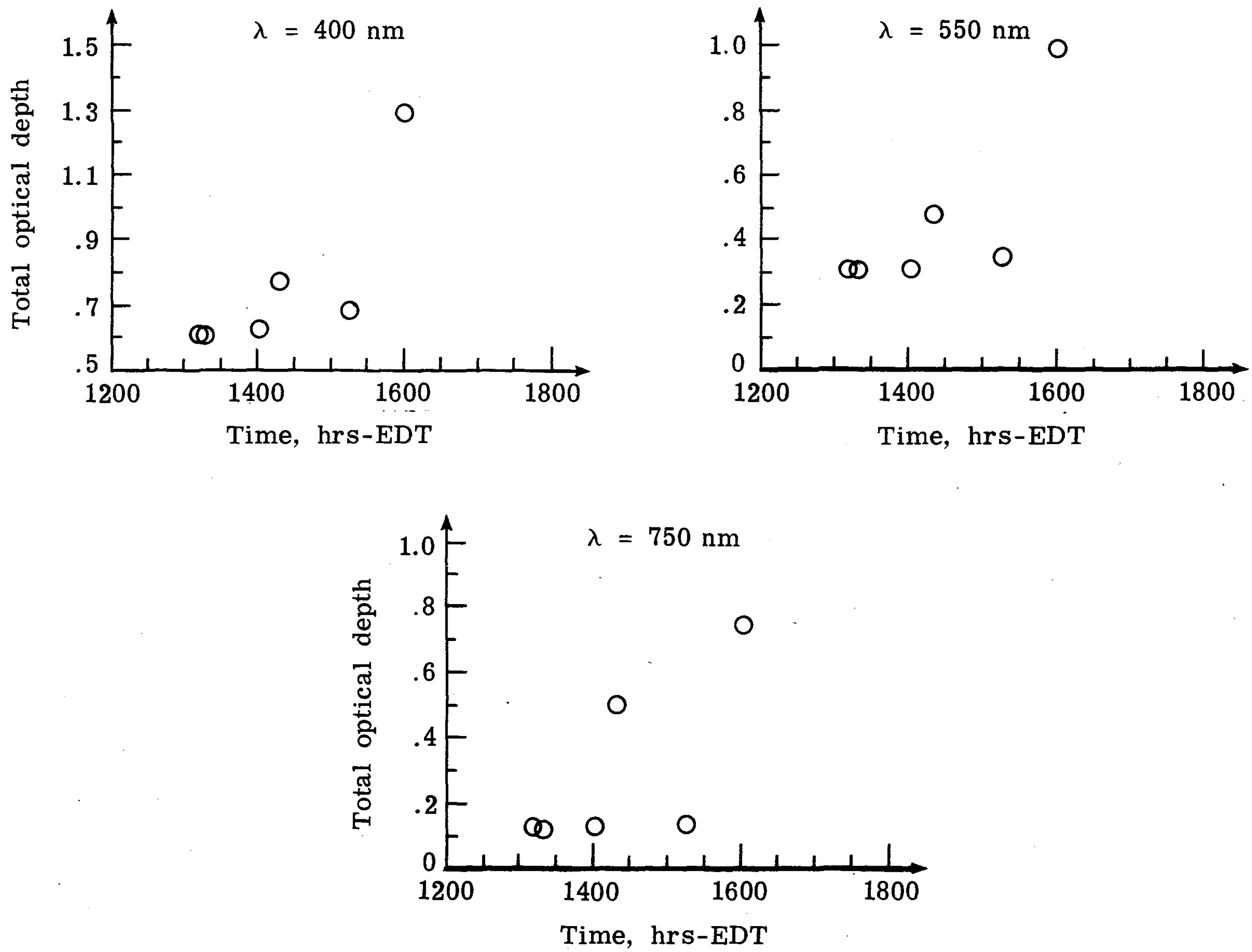

Figure 7(d).- Total optical depth histories for May 13, 1981.

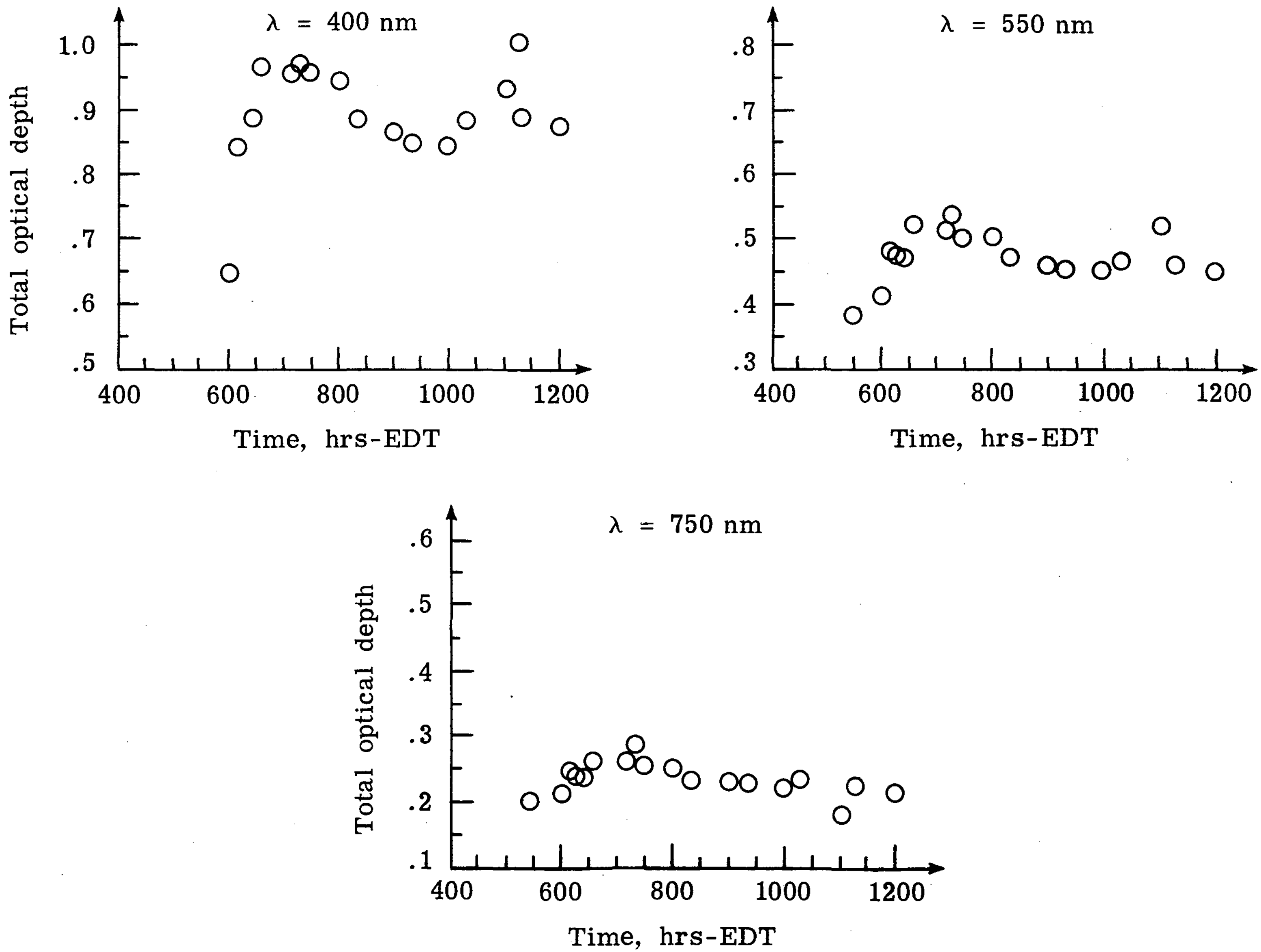

Figure 7(e). - Total optical depth histories for May 14, 1981.

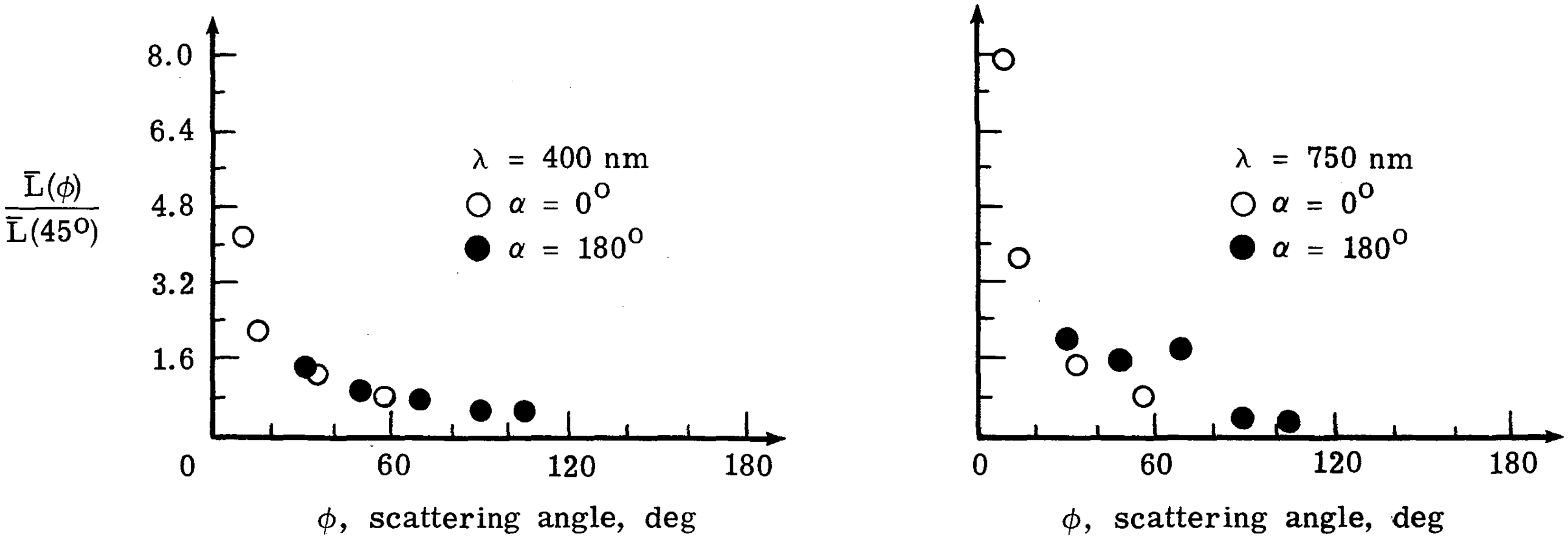

(a) Sun plane scan, May 7, 1335-1400 hrs-EDT.

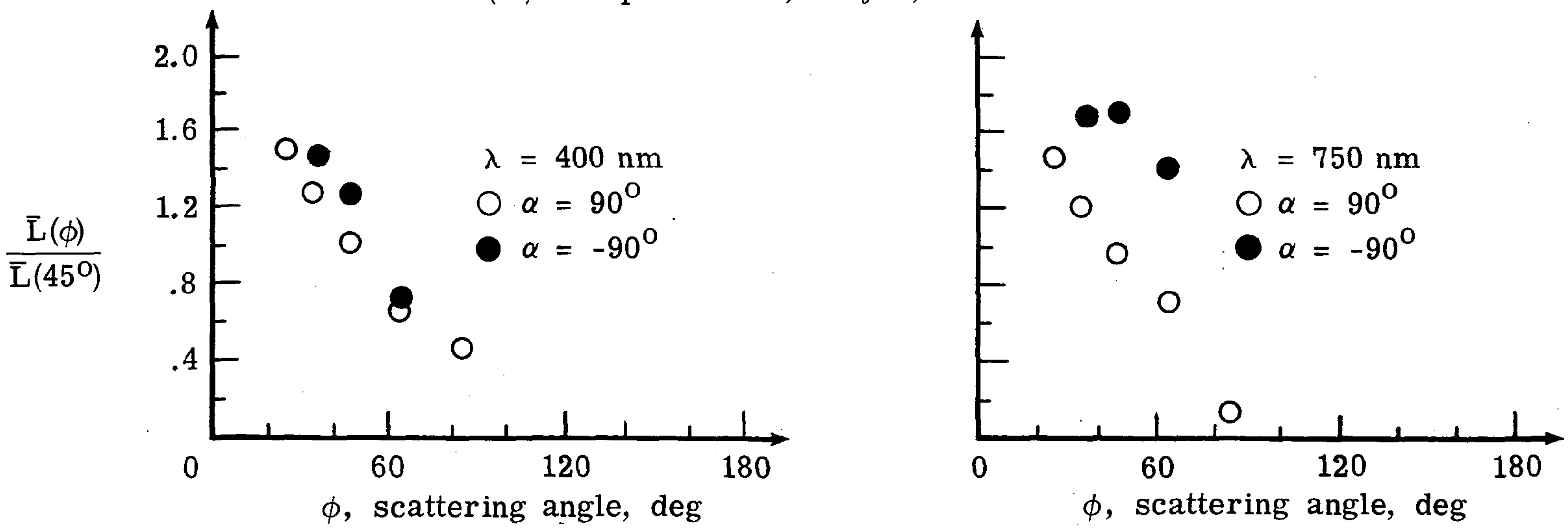

(b) Normal plane scan, May 7, 1240-1305 hrs-EDT.

Figure 8 (a), (b).- Normalized sky radiance distributions for May 7, 1981.

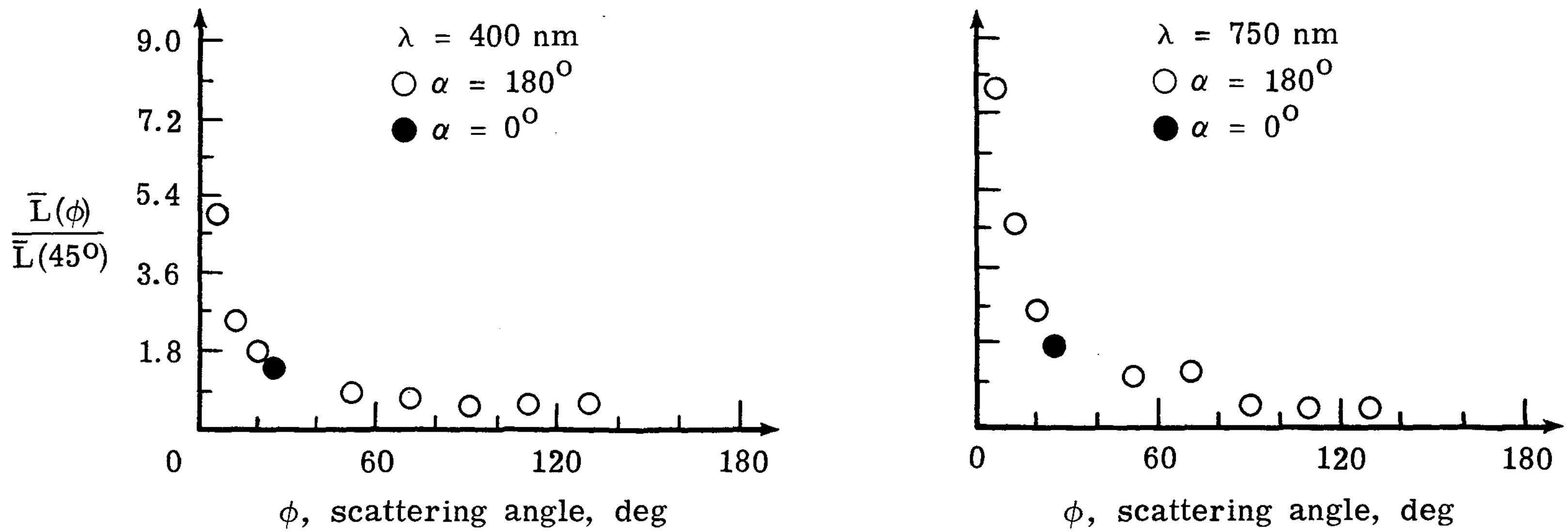

(c) Sun plane scan, May 8, 1556-1627 hrs-EDT

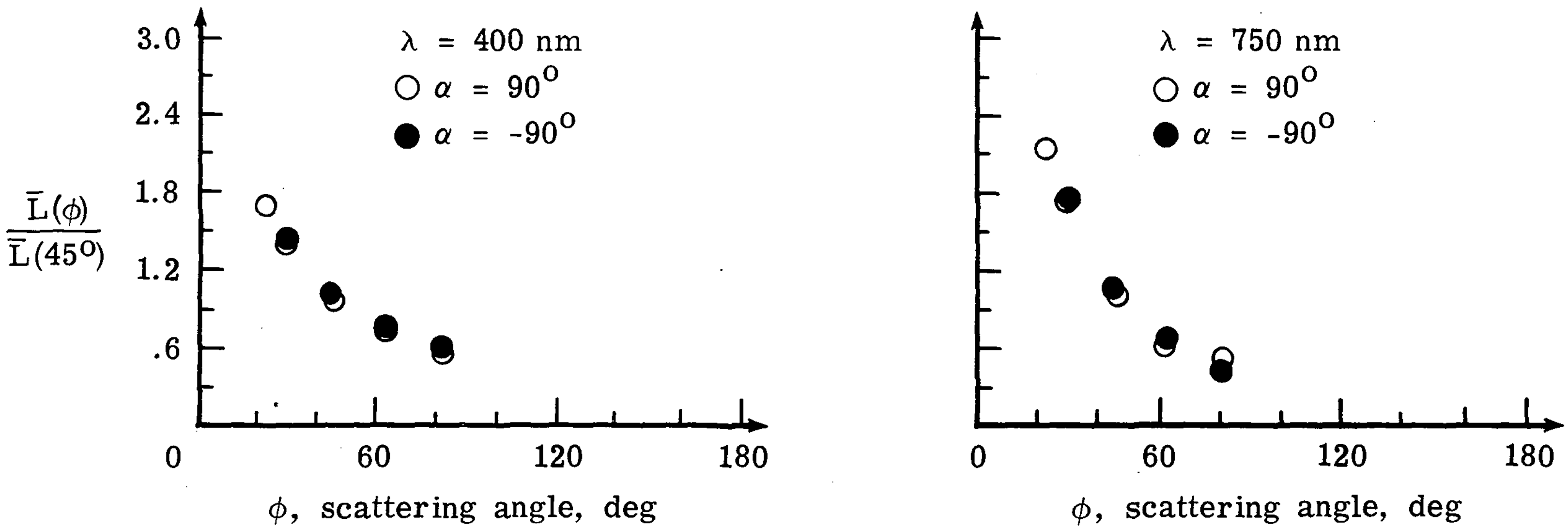

(d) Normal plane scan, May 13, 1229-1305 hrs-EDT

Figure 8(c), (d).- Normalized sky radiance distributions for May 8 and 13.

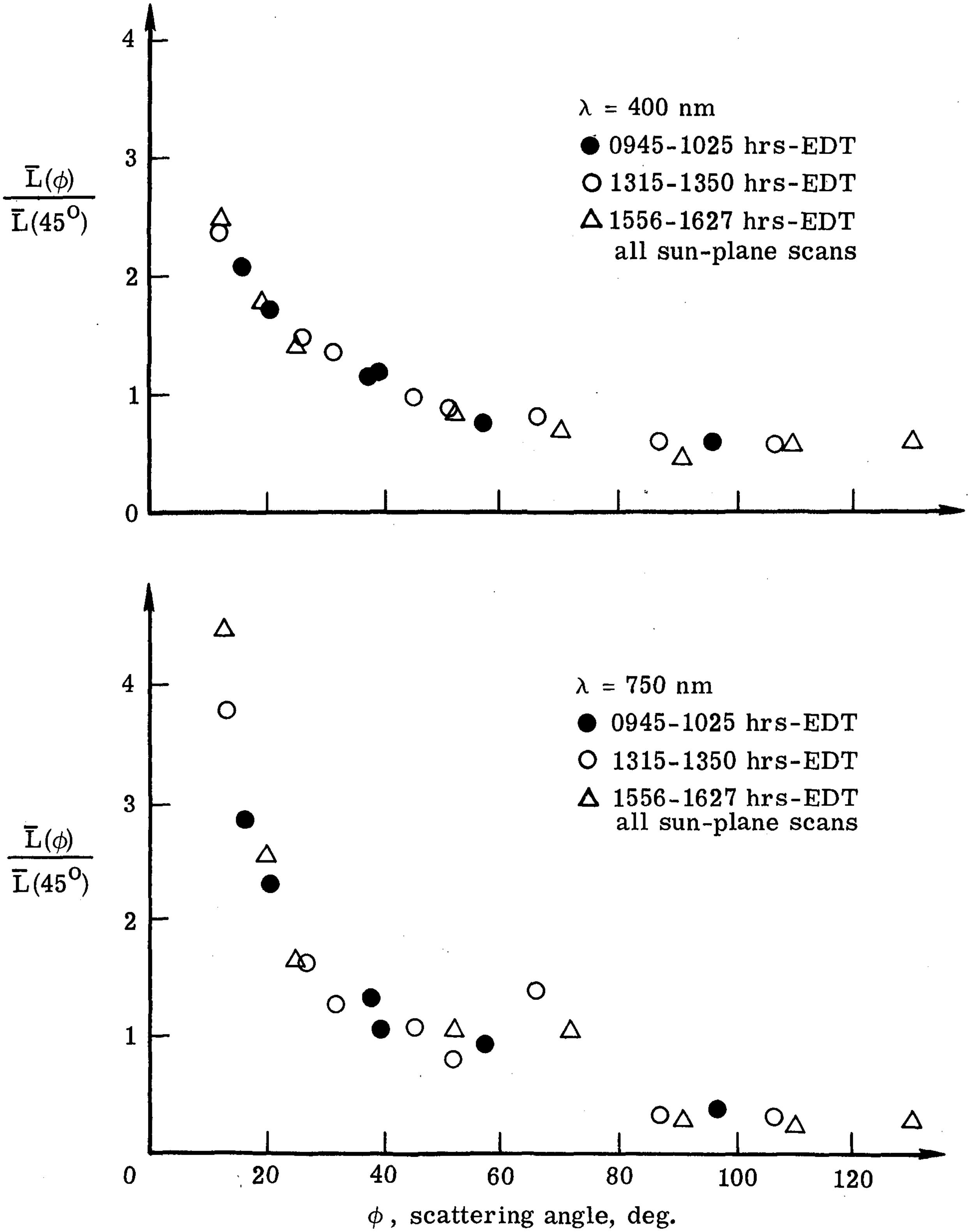

Figure 9. - Normalized sky radiance distributions for May 8, 1981.

1. Report No. NASA TM-83196	2. Government Accession No.	3. Recipient's Catalog No.
4. Title and Subtitle Spectral Atmospheric Observations at Nantucket Island, May 7-14, 1981		5. Report Date November 1981
		6. Performing Organization Code 146-40-15-07
7. Author(s) T. A. Talay and L. R. Poole		8. Performing Organization Report No.
9. Performing Organization Name and Address NASA Langley Research Center Hampton, Virginia 23665		10. Work Unit No.
		11. Contract or Grant No.
12. Sponsoring Agency Name and Address National Aeronautics and Space Administration Washington, DC 20546		13. Type of Report and Period Covered Technical Memorandum
		14. Sponsoring Agency Code
15. Supplementary Notes		

16. Abstract

During the period May 7-14, 1981, an experiment was conducted by the National Aeronautics and Space Administration, Langley Research Center, on Nantucket Island, Massachusetts, to measure atmospheric optical conditions using a 10-channel solar spectral photometer system. This experiment was part of a larger series of multidisciplinary experiments performed in the area of Nantucket Shoals aimed at studying the dynamics of phytoplankton production processes. Analysis of the collected atmospheric data yielded total and aerosol optical depths, transmittances, normalized sky radiance distributions, and total and sky irradiances. Results of this analysis may aid in atmospheric corrections of remote sensor data obtained by several sensors overflying the Nantucket Shoals area. Recommendations are presented concerning future experiments using the described solar photometer system and calibration and operational deficiencies uncovered during the experiment.

17. Key Words (Suggested by Author(s))	18. Distribution Statement
Remote Sensors Atmospheric Radiation Solar Radiation Atmospheric Observations	Unclassified - Unlimited Subject Category 43

19. Security Classif. (of this report)	20. Security Classif. (of this page)	21. No. of Pages	22. Price
Unclassified	Unclassified	55	A04

N-305

For sale by the National Technical Information Service, Springfield, Virginia 22161